
THE SUN AND THE HELIOSPHERE
AS AN INTEGRATED SYSTEM

THE SUN AND THE HELIOSPHERE AS AN INTEGRATED SYSTEM

Edited by

GIANNINA POLETTA

INAF, Osservatorio Astrofisico di Arcetri, Firenze, Italy

STEVEN T. SUESS

NSSTC, NASA Marshall Space Flight Center, Huntsville, Alabama, USA

Kluwer Academic Publishers
Boston/Dordrecht/London

A C.I.P. Catalogue record for this book is available from the Library of Congress.

ISBN 1-4020-2830-X (HB)
ISBN 1-4020-2831-8 (e-book)

Published by Kluwer Academic Publishers,
P.O. Box 17, 3300 AA Dordrecht, The Netherlands.

Sold and distributed in North, Central and South America
by Kluwer Academic Publishers,
101 Philip Drive, Norwell, MA 02061, U.S.A.

In all other countries, sold and distributed
by Kluwer Academic Publishers,
P.O. Box 322, 3300 AH Dordrecht, The Netherlands

All Rights Reserved
Copyright 2004 Kluwer Academic Publishers
No part of this work may be reproduced, stored in a retrieval system, or transmitted
in any form or by any means, electronic, mechanical, photocopying, microfilming, recording
or otherwise, without written permission from the Publisher, with the exception
of any material supplied specifically for the purpose of being entered
and executed on a computer system, for exclusive use by the purchaser of the work.

Contents

Preface	xi
1	
Hydrogen Walls: Mass Loss of Dwarf Stars and the Young Sun	1
<i>Jeffrey L. Linsky and Brian E. Wood</i>	
1 Is the Solar Wind Unique?	2
2 Hydrogen Walls: A New Tool for Measuring Mass-Loss Rates	6
2.1 Stellar Astrospheres	12
2.2 The Mass-Loss History of the Sun	17
3 Influence of Stellar Winds on Planets in the Solar System and Beyond	19
4 Conclusions	20
2	
The Heliospheric Interface: Models and Observations	23
<i>Vladislav V. Izmodenov</i>	
1 Introduction	23
2 Brief Summary of Observational Knowledge	26
2.1 Solar Wind Observations	26
2.2 Interstellar Parameters	27
3 Overview of Theoretical Approaches	29
3.1 H Atoms	30
3.2 Solar Wind and Interstellar Electron and Proton Components	32
3.3 Pickup Ions	34
3.4 Cosmic Rays	34
4 Overview of Heliospheric Interface Models	35
5 Self-Consistent Two-Component Model of the Heliospheric Interface and Recent Advancements of the Model	39
5.1 Plasma	39
5.2 H Atoms	42
5.3 Effects of Interstellar and Solar Wind Ionized Helium	45
5.4 Effects of GCRs, ACRs and the Interstellar Magnetic Field	47
5.5 Effects of the Solar Cycle Variations of the Solar Wind	49
5.6 Heliotail	52
6 Interpretations of Spacecraft Experiments Based on the Heliospheric Interface Model	53
6.1 Pickup ions	54
6.2 Location of the Termination Shock in the Direction of Voyager 1	56

	6.3	Filtration of Interstellar Oxygen and Nitrogen	57
7		Summary	57
3			
		Radiation from the Outer Heliosphere and Beyond	65
		<i>Iver H. Cairns</i>	
	1	Introduction	65
	2	Current Observational Status	68
	3	Basic Theoretical Issues	73
	4	The Priming/GMIR Theory	75
	5	Recent Theoretical Results	79
	6	Discussion and Conclusions	85
4			
		Ulysses at Solar Maximum	91
		<i>Richard G. Marsden</i>	
	1	Introduction	91
	2	Scientific Highlights at Solar Maximum	93
		2.1 Solar Wind	94
		2.2 Magnetic Field	99
		2.3 Energetic Particles	101
		2.4 Cosmic Rays	104
		2.5 Interstellar Dust	106
	3	The Future of Ulysses	107
5			
		Propagation of Energetic Particles to High Latitudes	113
		<i>T. R. Sanderson</i>	
	1	Introduction	113
	2	Solar Conditions	115
		2.1 Influence of the Sun on the Heliosphere	115
		2.2 Coronal Magnetic Field During a 22-year Solar Cycle	116
		2.3 Coronal Magnetic Field and Coronal Holes During the Ulysses Mission	119
	3	The First Orbit	120
	4	The Second Orbit	124
		4.1 The Second Polar Passes	125
	5	Discussion	129
		5.1 The Second Northern Polar Pass	129
		5.2 Comparison with the Second Southern Polar Pass	138
	6	Summary and Conclusions	141
6			
		Solar Wind Properties from IPS Observations	147
		<i>Masayoshi Kojima, Ken-ichi Fujiki, Masaya Hirano, Munetoshi Tokumaru, Tomoaki Ohmi and Kazuyuki Hakamada</i>	
	1	Introduction	148
	2	Interplanetary Scintillation Measurements	149
		2.1 Tomographic Analysis of IPS Observations	150
	3	Synoptic Velocity Maps	153
		3.1 Solar Cycle Dependence of Solar Wind Velocity Structure	155
	4	Correction Factor for CAT Analysis Results	155

<i>Contents</i>		vii
5	Coronal Hole Size Dependence of Solar Wind Velocity	158
6	Slow Solar Wind from a Small Coronal Hole	159
7	N-S Asymmetry of High-Latitude Fast Solar Wind	163
8	Velocity Gradient in High-Speed Region	165
9	Bimodal Structure of Solar Wind Velocity	167
10	Summary of Solar Cycle Dependence	170
11	Solar Wind Velocity and Physical Condition in Corona	170
	11.1 Data	171
	11.2 Cross-Correlation Analysis	172
12	Conclusion	174
7		
	The Dynamically Coupled Heliosphere	179
	<i>Nathan Schwadron</i>	
1	Introduction	179
2	Inner Source of Pickup Ions	181
3	Distant Cometary Tails	183
4	Outer Source of Pickup Ions and Anomalous Cosmic Rays	186
5	Ubiquitous Statistical Acceleration	187
6	Magnetic Footpoint Motions Through Speed Transitions and Resulting Particle Acceleration	189
7	FALTS	192
8	Summary	195
8		
	A Global Picture of CMEs in the Inner Heliosphere	201
	<i>N. Gopalswamy</i>	
1	Introduction	201
2	Solar Source of CMEs	202
3	CME Morphology	203
4	Physical Properties	206
5	Statistical Properties	207
	5.1 CME Speed	208
	5.2 CME Acceleration	208
	5.3 CME Width	211
	5.4 CME Latitude	211
	5.5 CME Occurrence Rate	212
	5.6 CME Mass and Energy	213
	5.7 Halo CMEs	215
6	Associated Activities	218
	6.1 Flares and CMEs	219
	6.2 Prominence Eruptions	220
	6.3 Are There Two types of CMEs?	221
	6.4 X-ray Ejecta	221
	6.5 CMEs and Radio Bursts	222
	6.6 CME Interaction and Radio Emission	225
7	CMEs and Solar Energetic Particles	226
8	CMEs in the Heliosphere	229
	8.1 High Latitude CMEs	231
9	CMEs and Solar Polarity Reversal	232
10	CMEs and Cosmic Ray Modulation	233
11	Some Outstanding Questions	236
	11.1 CME Initiation	236
	11.2 How do CMEs Evolve?	237

12	Summary	240
9	MHD Turbulence in the Heliosphere: Evolution and Intermittency	253
	<i>Bruno Bavassano, Roberto Bruno and Vincenzo Carbone</i>	
1	Introduction	254
2	MHD Turbulence Evolution	255
	2.1 Ecliptic Turbulence	256
	2.2 Polar Turbulence	258
	2.3 Conclusions on Turbulence Evolution	263
3	Intermittency	264
	3.1 Probability Distribution Functions of Fluctuations and Self-similarity	269
	3.2 Radial Evolution of Intermittency	271
	3.3 Identifying Intermittent Events	273
	3.4 Conclusions on Intermittency	277
10	Waves and Turbulence in the Solar Corona	283
	<i>Eckart Marsch</i>	
1	Introduction	284
2	Coronal Magnetic Field Structures	284
3	Magnetic Network Activity and Coronal Heating	287
4	Waves and Flows in Loops and Funnels	290
5	Magnetohydrodynamic Waves and Flux Tube Oscillations	293
	5.1 Observation and Theory	293
	5.2 Oscillations of Thin Flux Tubes	295
	5.3 Wave Amplitudes Versus Height from Numerical Models	298
	5.4 A Standing Slow Magnetoacoustic Wave	299
6	Plasma Waves and Heating of Particles	301
7	Generation, Transfer and Dissipation of Coronal Turbulence	303
	7.1 Generation of Magnetohydrodynamic Waves	303
	7.2 Wave Energy Transfer and Turbulent Cascade	304
	7.3 Wave Dissipation in the Kinetic Domain	307
	7.4 Origin and Generation of Coronal High-Frequency Waves	308
	7.5 Ion Velocity Distribution and Wave Absorption	310
8	Summary and Conclusion	313
11	The Influence of the Chromosphere-Corona Coupling on Solar Wind and Heliospheric Parameters	319
	<i>Øystein Lie-Svendsen</i>	
1	Introduction	320
2	Closed Coronal Loops	322
3	The Modelling Tools	325
4	The Electron-Proton Solar Wind	331
5	Helium in the Corona and Solar Wind	341
6	Summary	349
12	Elemental Abundances in the Solar Corona	353
	<i>John C. Raymond</i>	

<i>Contents</i>		ix
1	Introduction	353
2	Methods	355
	2.1 Coronal Observations	355
	2.2 Solar Wind Measurements	357
3	FIP Effect	357
	Flares	359
	Active regions	359
	Quiet Sun	360
	Coronal Holes	360
	Prominences	361
	Coronal Mass Ejections	361
	Average Coronal FIP Bias	361
	Solar Wind	362
4	Gravitational Settling	363
5	Comparison with Other Stars	366
6	Summary	367
13		
	The Magnetic Field from the Solar Interior to the Heliosphere	373
	<i>Sami K. Solanki</i>	
1	Introduction	373
2	Solar Interior	374
3	Solar Surface	375
4	Chromosphere and Corona	380
5	The Heliosphere	386
6	Conclusion	389
14		
	Magnetic Reconnection	397
	<i>E. R. Priest and D. I. Pontin</i>	
1	Introduction	397
2	Two-Dimensional Reconnection	399
	2.1 X-Collapse	399
	2.2 Sweet-Parker Reconnection	400
	2.3 Stagnation-Point Flow Model	401
	2.4 Petschek's Model	402
	2.5 More Recent Fast Mechanisms	403
3	Three-Dimensional Reconnection	405
	3.1 Structure of a Null Point	405
	3.2 Global Topology of Complex Fields	405
	3.3 3D Reconnection at a Null Point	407
4	Three-Dimensional Reconnection at an Isolated Non-Ideal Region	408
	4.1 Fundamental Properties of 3D Reconnection	409
	4.2 Analytical Solutions for 3D Reconnection	410
5	Heating the Solar Corona by Reconnection	412
	5.1 Converging Flux Model	413
	5.2 Binary Reconnection	413
	5.3 Separator Reconnection	414
	5.4 Braiding	414
	5.5 Coronal Tectonics	415
6	Reconnection in the Magnetosphere	416
	6.1 Dayside Reconnection	417
	6.2 Nightside Reconnection	418

x *THE SUN AND THE HELIOSPHERE AS AN INTEGRATED SYSTEM*

7 Conclusions

419

Chapter 2

THE HELIOSPHERIC INTERFACE: MODELS AND OBSERVATIONS

Vladislav V. Izmodenov

Moscow State University, Faculty of Mechanics and Mathematics

Department of Aeromechanics and Gas Dynamics

izmod@ipmnet.ru

Abstract The Sun is moving through a warm (~ 6500 K) and partly ionized local interstellar cloud (LIC) with velocity ~ 26 km/s. The charged component of the interstellar medium interacts with the solar wind (SW), forming the heliospheric interface - the SW/LIC interaction region. Both the solar wind and interstellar gas have a multi-component nature that creates a complex behavior in the interaction region. The current state of art in the modeling of the heliospheric interface is reviewed in this paper. Modern models of the interface take into account the solar wind and interstellar plasma components (protons, electrons, pickup ions, interstellar helium ions, and solar wind alpha particles), the interstellar neutral component (H atoms), interstellar and heliospheric magnetic fields, galactic and anomalous cosmic rays, and latitudinal and solar cycle variations of the solar wind. Predictions of self-consistent, time-dependent, kinetic/gasdynamic modeling of the heliospheric interface are compared with available remote diagnostics of the heliospheric interface - backscattered solar Lyman-alpha radiation, pickup ions, the deceleration of the solar wind at large heliocentric distances measured by Voyager 2, heliospheric absorption of stellar light, anomalous cosmic rays (ACRs), and heliospheric neutral atoms (ENAs).

Keywords: Solar Wind, Local Interstellar Cloud, Interstellar H atoms, Termination Shock

1. Introduction

The structure of the outer heliosphere and heliospheric boundary is determined by the interaction of the solar wind with the interstellar neighborhood of the Sun - the Local Interstellar Cloud (LIC). There is no

doubt that the LIC is partly ionized and that the charged component of the LIC interacts with solar wind plasma. The interaction region, which is often called the *heliospheric interface*, is formed in this interaction (Figure 1). The heliospheric interface is a complex structure, where the solar wind and interstellar plasma, interplanetary and interstellar magnetic fields, interstellar atoms of hydrogen, galactic and anomalous cosmic rays (GCRs and ACRs) and pickup ions play roles.

Although a space mission into the Local Interstellar Cloud is becoming now more realizable and Voyager 1 is approaching the inner boundary of the heliospheric interface – the termination shock, there are as yet no direct observations inside the heliospheric interface. Therefore, at the present time the heliospheric interface structure and local interstellar parameters can only be explored with remote and indirect measurements. Currently, the major sources of information on the heliospheric interface structure and position of the termination shock are following: 1) direct measurements of interstellar pickup ions, which are interstellar atoms ionized by charge exchange and photoionization and measured by Ulysses and ACE spacecraft; 2) anomalous cosmic rays, which are those pickup ions that are accelerated to high energies and measured by Voyagers, Pioneers, Ulysses, ACE, SAMPEX and Wind; 3) backscattered (by interstellar atoms of hydrogen) solar Lyman- α radiation measured at 1 AU by SOHO and Hubble Space Telescope (HST) and in the outer heliosphere by Voyager and Pioneer spacecraft; 4) direct measurements of the solar wind at large heliocentric distances by Voyager 2 spacecraft. In addition, kHz emission detected on board of Voyagers can provide other constraints (Cairns, this volume). Recently, it was shown that study of Ly- α absorptions toward nearby stars can serve as remote diagnostics of similar interfaces and, in particular, the hydrogen wall around heliopause-equivalents (see, Linsky and Wood, 1996; Wood et al., 2000; Izmodenov et al., 1999a, 2002; Linsky, this volume). First detections of heliospheric energetic atoms (ENAs) by SOHO and IMAGE proved that the detailed imaging of the heliospheric interface in ENAs will be possible in the near future (Gruntman et al., 2001; planned NASA IBEX mission: <http://ibex.swri.edu/>).

To reconstruct the structure of the interface and the physical processes inside the interface using remote observations at one to several astronomical units, a theoretical model should be employed. Theoretical studies of the heliospheric interface have been performed for more than four decades, following the pioneering papers by Parker (1961) and Baranov et al. (1971). However, a complete theoretical model of the heliospheric interface has not yet been constructed. The difficulty in doing this is connected with the multi-component nature of both the LIC and the

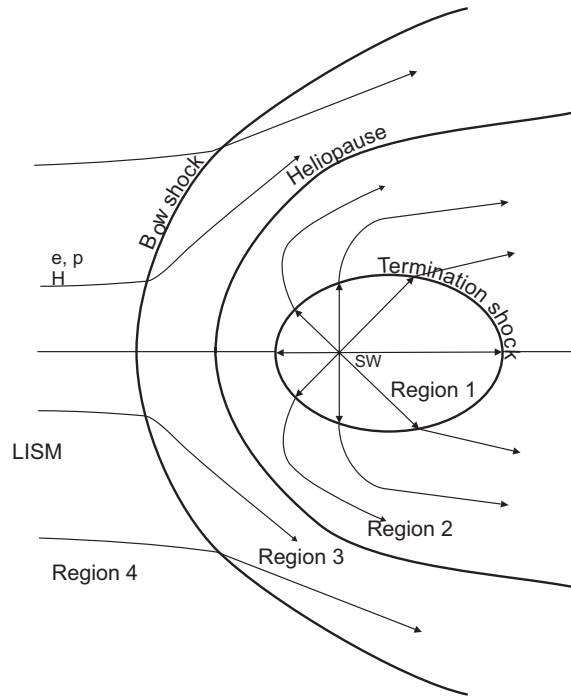


Figure 2.1 The heliospheric interface is the region of the solar wind interaction with LIC. The heliopause is a contact discontinuity, which separates the plasma of the solar wind from the interstellar plasma. The termination shock decelerates the supersonic solar wind. The bow shock may also exist in the supersonic interstellar wind. The heliospheric interface is thus divided into four regions: 1) supersonic solar wind; 2) subsonic solar wind in the region between the heliopause and termination shock; 3) disturbed interstellar plasma region (or “pile-up” region) around the heliopause; 4) undisturbed interstellar medium.

solar wind. The LIC consists of at least five components: plasma (electrons and protons), hydrogen atoms, interstellar magnetic field, galactic cosmic rays, and interstellar dust. The heliospheric plasma consists of original solar particles (protons, electrons, alpha particles, etc.), pickup ions and the anomalous cosmic ray component. Pickup ions modify the heliospheric plasma flow starting from ~ 20 -30 AU. ACRs may also modify the plasma flow upstream of the termination shock and in the heliosheath. Spectra of ACRs can serve as remote diagnostics of the termination shock (Stone, 2001). For a recent review on ACRs see Fichtner (2001).

Development of a theoretical model of the heliospheric interface requires choosing a specific approach for each of interstellar and solar wind component. Interstellar and solar wind protons and electrons can be described as fluids. At the same time the mean free path of interstellar H atoms is comparable with the size of the heliospheric interface. This requires kinetic description for the interstellar H atom flow in the interaction region. For the pickup ion and cosmic ray components the kinetic approach is also required.

This chapter focuses on 1) theoretical numerical models of the *global* heliospheric interface structure and 2) application of the models to interpreting different remote diagnostics of the SW/LIC interaction. Under global models I include those models that describe the entire interaction region, including the termination shock, the heliopause and possible bow shock. In this sense, this chapter should not be considered as a complete review of progress in the field. Many different approaches have been used to look into different aspects of the solar wind interaction with LIC connected with pickup ion transport and acceleration, with the termination shock structure under influence of ACRs, and pickup ions. For a more complete overview see recent reviews Zank (1999a), Fichtner (2001).

The structure of the chapter is the following: The next section briefly describes our current knowledge of the local interstellar and solar wind parameters. Section 3 discusses theoretical approaches to be used for the interstellar and solar wind components. Section 4 gives an overview of heliospheric interface models. Section 5 describes basic results of self-consistent two-component model of the heliospheric interface developed in Moscow and its recent developments. In section 6 we demonstrate possible analysis of space experiments on the basis of a theoretical model of the heliospheric interface. Section 7 gives a summary and underlines current problems in the modeling of the global heliosphere and discusses future perspectives.

2. Brief Summary of Observational Knowledge

Choice of an adequate theoretical model of the heliospheric interface depends on boundary conditions, i.e. on the undisturbed solar wind and interstellar properties.

2.1 Solar Wind Observations

At the Earth's orbit, the flux of the interstellar atoms is quite small and the solar wind can be considered undisturbed. Measurements of pickup ions and ACRs also show that these components do not have dynamical influences on the original solar wind particles at the Earth's orbit. Therefore, the Earth's orbit can be taken as inner boundary of the SW/LIC interaction problem.

Solar wind structure and behavior evolves over a solar cycle (e.g., Gazis, 1996; Neugebauer 1999; McComas et al. 2000, 2001, 2002). At solar minima, high-latitude regions on the Sun have well-developed coronal holes, which are sources of high-speed (~ 700 km/s), low-density solar wind. At low heliolatitudes the solar wind has low speed (~ 400 km/s) and high density. The dividing line between the fast and slow solar wind

regimes is at about 20° heliolatitude. At solar maximum the slow, dense solar wind is present at all latitudes (McComas et al., 2002). Shortly after the solar maximum coronal holes and, therefore, the high-speed solar wind appear again. At this stage, both coronal holes the high-speed solar wind may appear even in the ecliptic, which results in increasing the average solar wind momentum flux at low latitudes shortly after solar maxima. Spacecraft near the ecliptic at 1 AU have detected variations of the solar wind momentum flux by a factor of two (Lazarus and McNutt, 1990; Gazis, 1996). Deep space probe data obtained with Pioneer and Voyager measurements in the distant solar wind also support this conclusion (Lazarus and McNutt, 1990; Gazis, 1996). A recent update of the Voyager 2 measurements of the solar wind can be found in Richardson et al. (2004). Apparently, over the past two solar cycles the momentum flux had a minimum value at solar maximum, then increased rapidly after solar maximum reaching a peak 1-2 years later. The pressures subsequently decreased until after the next solar maximum. It was unclear from the measurements in the ecliptic whether the variations of the momentum flux have global effect or limited to the ecliptic. Ulysses observations from its first full polar orbit showed that the momentum flux is diminished near the equator compared to higher latitudes. The effect is clearly evident in the period near solar minimum (May, 1995 - December, 1997) (McComas et al., 2000). Around solar maximum the three-dimensional structure of the solar wind is remarkably different from, and more complicated than, the simple, bimodal structure observed throughout much of the rest of the solar cycle. At maximum, the solar wind has the same properties at all latitudes (McComas et al., 2001, 2002).

Theoretical models predict that pickup and ACR components dynamically influence the solar wind at large heliocentric distances. Table 2.1 presents estimates of dynamic importance of the heliospheric plasma components at small and large heliocentric distances. The table shows that pickup ion thermal pressure can be up to 30-50 % of the dynamic pressure of solar wind.

2.2 Interstellar Parameters

Local interstellar temperature and velocity can be inferred from direct measurements of interstellar helium atoms by the Ulysses/GAS instrument (Witte et al., 1996; Witte, 2004). Atoms of interstellar helium penetrate the heliospheric interface undisturbed, because of the small strength of their coupling with interstellar and solar wind protons. Indeed, due to small cross sections of elastic collisions and charge exchange

Table 2.1. Number Densities and Pressures of Solar Wind Components

Component	4-5 AU		80 AU	
	Number Density cm^{-3}	Pressure eV/cm^{-3}	Number Density cm^{-3}	Pressure eV/cm^{-3}
Original solar wind protons	0.2-0.4	2.-4. (thermal) ~ 200 (dynamic)	$(7 - 14) \cdot 10^{-4}$	$10^{-3} - 10^{-4}$ $\sim 0.5 - 1.$ (dynamic)
Pickup ions Anomalous cosmic rays	$5.1 \cdot 10^{-4}$	0.5	$\sim 2 \cdot 10^{-4}$	~ 0.15 0.01 - 0.1

Table 2.2. Local Interstellar Parameters

Parameter	Direct measurements/estimations
Sun/LIC relative velocity	$25.3 \pm 0.4 \text{ km s}^{-1}$ (direct He atoms ¹) 25.7 km s^{-1} (Doppler-shifted absorption lines ²)
Local interstellar temperature	$7000 \pm 600 \text{ K}$ (direct He atoms ¹) 6700 K (absorption lines ²)
LIC H atoms number density	$0.2 \pm 0.05 \text{ cm}^{-3}$ (estimate based on pickup ion observations ³)
LIC proton number density	$0.03 - 0.1 \text{ cm}^{-3}$ (estimate based on pickup ion observations ³)
Local Interstellar magnetic field	Magnitude: 2-4 μG Direction: unknown
Pressure of low energetic part of cosmic rays	$\sim 0.2 \text{ eV cm}^{-3}$

¹ Witte et al. (1996); ² Lallement(1996); ³ Gloeckler (1996), Gloeckler et al. (1997)

with protons, the mean free path of these atoms is larger than the heliospheric interface. Independently, the velocity and temperature in the Local Interstellar Cloud can be deduced from analysis of absorption features in the stellar spectra (Lallement, 1996). However, this method provides mean values along lines of sight toward nearby stars in the LIC. A comparison of local interstellar temperatures and velocities derived from stellar absorption with those derived from direct measurements of interstellar helium shows quite good agreement (see Table 2.2).

Other local parameters of the interstellar medium, such as interstellar H atom and electron number densities, and strength and direction of the interstellar magnetic field, are not well known. In the models they can be considered as free parameters. However, indirect measurements of interstellar H atoms and direct measurements of their derivatives as pickup ions and ACRs provide important constraints on the local interstellar proton and atom densities and total interstellar pressure. The neutral H density in the inner heliosphere depends on filtration

of the neutral H atoms in the heliospheric interface due to charge exchange. Since interstellar He is not perturbed in the interface, the local interstellar number density of H atoms can be estimated from the neutral hydrogen to the neutral helium ratio in the LIC, $R(HI/HeI)_{LIC}$: $n_{LIC}(HI) = R(HI/HeI)_{LIC}n_{LIC}(HeI)$. The neutral He number density in the heliosphere has been recently determined to be very likely around $0.015 \pm 0.002 \text{ cm}^{-3}$ (Gloeckler and Geiss, 2001). The interstellar ratio HI/HeI is likely in the range of 10-14. Therefore, expected interstellar H atom number densities are in the range of $0.13 - 0.25 \text{ cm}^{-3}$. It was shown by modeling (Baranov and Malama, 1995; Izmodenov et al., 1999b) that the filtration factor, which is the ratio of neutral H density inside and outside the heliosphere, is a function of interstellar plasma number density. Therefore, the number density of interstellar protons (electrons) can be estimated from this filtration factor (Lallement, 1996). Independently, the electron number density in the LIC can be estimated from abundances ratios of ions of different ionization states (Lallement, 1996).

Note that there are other methods to estimate interstellar H atom density inside the heliosphere, based on their influence on the distant solar wind (Richardson, 2001) or from ACR spectra (Stone, 2001). Recent estimates of the location of the heliospheric termination shock using transient decreases of cosmic rays observed by Voyager 1 and 2 also provide constraints on the local interstellar parameters (Webber et al., 2001). However, simultaneous analysis of different types of observational constraints has not been done yet. Theoretical models should be employed to make such analysis. Table 2.2 presents a summary of our knowledge of local interstellar parameters. Using these parameters, we estimate local pressures of different interstellar components (Table 1.3). Although the dynamical pressure of interstellar H atoms is larger than all other pressures, all pressures have the same order of magnitude. This means that theoretical models should not neglect any of these interstellar components. A portion of the H atoms, ACRs and GCRs penetrates into the heliosphere, which makes their real dynamical influence on the heliospheric plasma interface difficult to estimate.

3. Overview of Theoretical Approaches

In this section we consider theoretical approaches for components involved in the dynamical processes in the heliospheric interface.

Generally, any gas can be described on a kinetic or a hydrodynamic level. In the kinetic approach, macroscopic parameters of a gas of s -particles (or, briefly, s -gas) can be expressed through integrals of the ve-

Table 2.3. Local Pressures of Interstellar Components

Component	Pressure estimation, dyn cm ⁻²
Interstellar plasma component	
Thermal pressure	(0.6 – 2.0) · 10 ⁻¹³
Dynamic pressure	(1.5 – 6) · 10 ⁻¹³
H atoms	
Thermal pressure	(0.6 – 2.0) · 10 ⁻¹³
Dynamic pressure	(4.0 – 9.0) · 10 ⁻¹³
Interstellar magnetic field	(1.0 – 5.0) · 10 ⁻¹³
Low energy part of GCR	(1.0 – 5.0) · 10 ⁻¹³

locity distribution function $f_s(\vec{r}, \vec{w}, t)$: $n_s = \int f_s d\vec{w}$, $\vec{V}_s = (\int \vec{w} f_s d\vec{w})/n_s$, $P_{s,ij} = m_s \int (w_i - V_{s,i})(w_j - V_{s,j}) f_s d\vec{w}$, $\vec{q}_s = 0.5 m_s \int (\vec{w} - \vec{V}_s)^2 (\vec{w} - \vec{V}_s) f_s d\vec{w}$, where n_s is the number density of s -gas, \vec{V}_s is the bulk velocity of s -gas, $P_{s,ij}$ are components of the stress tensor \hat{P}_s , \vec{q}_s is the thermal flux vector, and m_s is the mass of individual s -particle. In the hydrodynamic approach, some assumptions should be made to specify the stress tensor, \hat{P}_s , and the thermal flux vector, \vec{q}_s to make hydrodynamic system closed. For example, these values can be calculated by the Chapman-Enskog method, assuming $Kn = l/L \ll 1$, where l and L are the mean free path of the particles and characteristic size of the problem, respectively. The zero approximation of the Chapman-Enskog method gives local Maxwellian distribution, and the gas can be considered as an ideal gas, where the stress tensor reduces to scalar pressure P and $\vec{q} = 0$.

3.1 H Atoms

Interstellar atoms of hydrogen form the most abundant component in the circumsolar local interstellar medium (see, Table 2.2). These atoms penetrate deep into the heliosphere and interact with interstellar and solar wind protons. The cross sections of elastic H-H, H-p collisions are negligible as compared with the charge exchange cross section (Izmodenov et al., 2000). Charge exchange with solar wind/interstellar protons determines the properties of the H atom gas in the interface. Atoms, newly created by charge exchange, have the local properties of protons. Since plasma properties are different in the four regions of the heliospheric interface shown in Figure 1, the H atoms can be separated into four populations, each having significantly different properties. The strength of H atom-proton coupling can be estimated through the calculation of the mean free path of H atoms in the plasma. Generally, the

mean free path (with respect to the momentum transfer) of an s-particle in a t-gas can be calculated by the formula: $l = m_s w_s^2 / (\delta M_{st} / \delta t)$. Here, w_s is the individual velocity of the s-particle, and $\delta M_{st} / \delta t$ is the individual s-particle momentum transfer rate in the t-gas.

Table 2.4 shows the mean free paths of H atoms with respect to charge exchange with protons. The mean free paths are calculated for typical atoms of different populations in different regions of the interface in the upwind direction. For every population of H atoms, there is at least one region in the interface where the Knudsen number $Kn \approx 0.5 - 1.0$. Therefore, the kinetic Boltzmann approach must be used to describe interstellar atoms in the heliospheric interface correctly.

Table 2.4. Mean free paths of H-atoms in the heliospheric interface with respect to charge exchange with protons, in AU.

Population	At TS	At HP	Between HP and BS	LISM
4 (primary interstellar)	150	100	110	870
3 (secondary interstellar)	66	40	58	190
2 (atoms originating in the heliosheath)	830	200	110	200
1 (neutralized solar wind)	16000	510	240	490

The velocity distribution of H atoms $f_H(\vec{r}, \vec{w}_H, t)$ may be calculated from the linear kinetic equation:

$$\begin{aligned} \frac{\partial f_H}{\partial t} + \vec{w}_H \cdot \frac{\partial f_H}{\partial \vec{r}} + \frac{\vec{F}}{m_H} \cdot \frac{\partial f_H}{\partial \vec{w}_H} = -f_H \int |\vec{w}_H - \vec{w}_p| \sigma_{ex}^{HP} f_p(\vec{r}, \vec{w}_p) d\vec{w}_p \\ + f_p(\vec{r}, \vec{w}_H) \int |\vec{w}_H^* - \vec{w}_H| \sigma_{ex}^{HP} f_H(\vec{r}, \vec{w}_H^*) d\vec{w}_H^* - (\nu_{ph} + \nu_{\text{impact}}) f_H(\vec{r}, \vec{w}_H). \end{aligned} \quad (2.1)$$

Here $f_H(\vec{r}, \vec{w}_H)$ is the distribution function of H atoms; $f_p(\vec{r}, \vec{w}_p)$ is the local distribution function of protons; \vec{w}_p and \vec{w}_H are the individual proton and H atom velocities, respectively; σ_{ex}^{HP} is the charge exchange cross section of an H atom with a proton; ν_{ph} is the photoionization rate; m_H is the atomic mass; ν_{impact} is the electron impact ionization rate; and \vec{F} is the sum of the solar gravitational force and the solar radiation pressure force. The plasma and neutral components interact mainly by charge exchange. However, photoionization, solar gravitation, and radiation pressure, which are taken into account in equation (2.1), are important at small heliocentric distances. Electron impact ionization may be important in the heliosheath (region 2). The interaction of the plasma and H atom components leads to the mutual exchanges of mass, momentum and energy. These exchanges should be taken into account

in the plasma equations through source terms, which are integrals of $f_H(\vec{r}, \vec{w}, t)$ specified later in equations (1.5)-(1.7).

3.2 Solar Wind and Interstellar Electron and Proton Components

Basic assumptions necessary to employ a hydrodynamic approach for space plasmas were reviewed by Baranov (2000). In particular, it was concluded there that interstellar and solar wind plasmas can be treated hydrodynamically. Indeed, the mean free path of charged particles in the local interstellar plasma is less than 1 AU, which is much smaller than the size of the heliospheric interface itself. Therefore, the local interstellar plasma is a collisional plasma, and a hydrodynamic approach can be used to describe it. Solar wind plasma is collisionless, because the mean free path of the solar wind particles with respect of coulomb collisions is much larger than the size of the heliopause. Therefore, the heliospheric termination shock (TS) is a collisionless shock. A hydrodynamic approach can be justified for collisionless plasmas when scattering of charged particles on plasma fluctuations is efficient (“collective plasma processes”). In this case, the mean free path l with respect to collisions is replaced by l_{coll} , the mean free path of collective processes, which is assumed to be less than the characteristic length of the problem L : $l_{coll} \ll L$. However, the integral of “collective collisions” is too complicated to be used to calculate the transport coefficient for collisionless plasmas.

A one-fluid description of heliospheric and interstellar plasmas is commonly used in the global models of the heliospheric interface. Governing equations of the one-fluid approach are mass, momentum and energy balance equations:

$$\frac{\partial \rho}{\partial t} + \nabla \cdot (\rho \vec{V}) = q_1, \quad (2.2)$$

$$\frac{\partial(\rho \vec{V})}{\partial t} + \nabla P + \nabla \cdot (\rho \vec{V} \otimes \vec{V}) - \frac{1}{4\pi} [rot \vec{B} \times \vec{B}] = -\nabla P_{cr} + \vec{q}_2 \quad (2.3)$$

$$\frac{\partial}{\partial t} \left(\frac{3}{2} P \right) + \nabla \cdot \left(\frac{5}{2} P \vec{V} \right) - \vec{V} \cdot \nabla P = q_3 - \vec{q}_2 \cdot \vec{V} - \vec{V} \cdot \nabla P_{cr} \quad (2.4)$$

Here $\rho = m_p(n_p + n_{pui})$; $P = P_e + P_p + P_{pui}$; P_e , P_p , P_{pui} and P_{cr} are pressures of electrons, protons, pickup ions and cosmic rays, respectively; q_1 , \vec{q}_2 and q_3 are source terms in the plasma due to the charge exchange process with H atoms, photoionization and electron impact ionization:

$$q_1 = m_p n_H (\nu_{ph} + \nu_{impact}) \quad (2.5)$$

$$\begin{aligned}
\vec{q}_2 = & m_p \int (\nu_{ph} + \nu_{impact}) \vec{v}_H f_H(\vec{v}_H) d\vec{v}_H + \\
& m_p \int \int u \sigma_{ex}^{HP}(u) (\vec{w}_H - \vec{w}_p) f_H(\vec{w}_H) f_p(\vec{w}_p) d\vec{w}_H d\vec{w}_p + \\
& m_p \int \int u \sigma_{ex}^{HP}(u) (\vec{w}_H - \vec{w}_i) f_H(\vec{w}_H) f_{pui}(\vec{w}_i) d\vec{w}_H d\vec{w}_i
\end{aligned} \tag{2.6}$$

$$\begin{aligned}
q_3 = & m_p \int (\nu_{ph} + \nu_{impact}) \frac{\vec{w}_H^2}{2} f_H(\vec{w}_H) f_p(\vec{w}_p) d\vec{w}_p d\vec{w}_H \\
& + m_p \int \int u \sigma_{ex}^{HP}(u) \frac{\vec{w}_H^2 - \vec{w}_p^2}{2} f_H(\vec{w}_H) f_p(\vec{w}_p) d\vec{w}_p d\vec{v}_H \\
& + m_p \int \int u \sigma_{ex}^{HP}(u) \frac{\vec{w}_H^2 - \vec{w}_i^2}{2} f_H(\vec{w}_H) f_{pui}(\vec{w}_i) d\vec{w}_i d\vec{w}_H
\end{aligned} \tag{2.7}$$

Here f_p is the Maxwellian velocity distribution of the solar wind and interstellar protons and f_{pui} is the velocity distribution of the pickup ions, which should be determined by a solution of the pickup ion kinetic transport equation or by assumption of complete assimilation of pickup ions into the solar wind plasma.

Faraday's equation

$$\frac{\partial \vec{B}}{\partial t} = rot[\vec{v} \times \vec{B}] \tag{2.8}$$

should be added to the system of governing equations (2.2)-(2.4) to make the system closed. This form of Faraday's equation follows from the classical form of the Ohm's law in the case of ideal conductivity: $\vec{E} = -\frac{1}{c}[\vec{V} \times \vec{B}]$.

Governing equations (2.2)-(2.8) for the one-fluid approach are obtained by summarizing mass, momentum and energy balance equations for electrons, protons and pickup ions under certain assumptions, which were recently discussed by Baranov and Fahr (2003a,b) and Florinsky et al. (2003). Ideal MHD equations with source terms q_1 , \vec{q}_2 , q_3 in the right-hand sides were solved self-consistently with equation (2.1) by Aleksashov et al. (2000) in the case when the IS magnetic field is parallel to the interstellar flow.

To derive the classical system of hydrodynamic equations applied for heliospheric interface in one-fluid models, one needs to ignore terms containing magnetic and electric fields in equations (2.3) and (2.4). In this case, equations (2.2)-(2.4) together with kinetic equation (2.1) for H atoms and expressions (1.5)-(1.7) for the source terms q_1 , \vec{q}_2 and q_3 form a closed system of equations.

3.3 Pickup Ions

To study pickup ion evolution in the outer heliosphere and in the heliospheric interface, details of the process of charged particle assimilation into the magnetized plasma are needed. A newly created ion under the influence of the large scale solar wind electric and magnetic fields executes a cycloidal trajectory with the guiding center drifting at the bulk velocity of the solar wind. Assuming that the gyroradius is much smaller than the typical scale length, one can average the velocity distribution function over the gyrotory motion. The initial ring-beam distribution of pickup ions is unstable. Basic processes that determine evolution of the pickup ion distribution are pitch-angle scattering, convection, adiabatic cooling in the expanding solar wind, injection of newly ionized particles, and energy diffusion in the wave field of both the solar wind and that generated by pickup ions and different kinds of instabilities of waves in the solar wind. The most general form of the relevant transport equation describing the evolution of gyrotropic velocity distribution function $f_{pui} = f_{pui}(t, \vec{r}, v, \mu)$ of pickup ions in a background plasma moving at a velocity \vec{V}_{sw} was written by Isenberg (1997) and Chalov and Fahr (1998). f_{pui} is a function of the modulus of velocity in the solar wind rest frame, and μ is the cosine of pitch angle.

Theoretical models show (section 5) that the assumption of complete assimilation of pickup ions into the solar wind would lead to a great increase of plasma temperature with the heliocentric distance. Since such an increase is not observed, the solar wind and pickup protons represent two distinct proton populations up to the TS. Nevertheless, the radial temperature profile of protons measured by Voyager 2 shows a smaller decrease than predicted by adiabatic cooling. A fraction of the heating of solar wind protons may thus be connected with pickup generated waves (Williams et al., 1995; Smith et al., 2001). Many aspects of pickup ion evolution have been studied (e.g., Chalov and Fahr, 1999; for reviews, see Zank, 1999a; Fichtner, 2001). However, to date detailed models of the assimilation process of pickup ions into the solar wind have not been taken into account in the global models of the heliospheric interface structure.

3.4 Cosmic Rays

Cosmic rays are coupled to background flow via scattering by plasma waves. The net effect is that the cosmic rays tend to be convected along with the background plasma as they diffuse through the magnetic irregularities carried by the background plasma. Both galactic and anomalous cosmic rays can be treated as populations with negligible mass density

but non-negligible high energy density. At a hydrodynamical level, the cosmic rays may modify the wind flow via their pressure gradient ∇P_c , with the net energy transfer rate from fluid to the cosmic rays given by $\vec{V} \cdot \nabla P_c$. $P_c(\vec{r}, t) = \frac{4\pi}{3} \int_0^\infty f_c(\vec{r}, p, t) w p^3 dp$ is a cosmic ray pressure and $f_c(\vec{r}, p, t)$ is the isotropic velocity distribution of cosmic rays.

The transport equation of cosmic rays has the following form (e.g., Fichtner, 2001):

$$\frac{\partial f_c}{\partial t} = \frac{1}{p^2} \frac{\partial}{\partial p} \left(p^2 D \frac{\partial f_c}{\partial p} \right) + \nabla \cdot (\hat{k} \nabla f_c) - \vec{V} \cdot \nabla f_c + \frac{1}{3} (\nabla \cdot \vec{V}) \frac{\partial f_c}{\partial \ln p} + S(\vec{r}, p, t) \quad (2.9)$$

Here p is the modulus of the momentum of the particle; D is the diffusion coefficient in momentum space, often assumed to be zero; \hat{k} is the tensor of spatial diffusion; $\vec{V} = \vec{U} + \vec{V}_{drift}$ is the convection velocity; \vec{U} is the plasma bulk velocity; \vec{V}_{drift} is a drift velocity in the heliospheric or interstellar magnetic field; and $S(\vec{r}, p, t)$ is the source term.

At the hydrodynamic level, the transport equation of the cosmic rays is:

$$\frac{\partial P_c}{\partial t} = \nabla \cdot [\hat{k} \nabla P_c - \gamma_c (\vec{U} + U_{dr}) P_c] + (\gamma_c - 1) \vec{U} \cdot \nabla P_c + Q_{acr,pui}(\vec{r}, t) \quad (2.10)$$

The last equation assumes that $D = 0$; U_{dr} is momentum-averaged drift velocity; γ is the polytropic index; and $Q_{acr,pui}$ is the energy injection rate describing energy gains of the ACRs from pickup ions. Chalov and Fahr (1996, 1997) suggested that $Q_{acr,pui} = -\alpha p_{pui} \nabla \cdot \vec{U}$, where α is a constant injection efficiency defined by the specific plasma properties (Chalov and Fahr, 1997). α is set to zero for GCRs since no injection occurs into the GCR component.

4. Overview of Heliospheric Interface Models

A complete model of the SW/LIC interaction has not yet been developed. However, in recent years, several groups have focused their efforts on theory and modeling of the heliospheric interface in order to understand influence of one (or several) components on the interface separately from others. In particular, the influence of the magnetic fields on the interface structure was studied in Fujimoto and Matsuda (1991), Baranov and Zaitsev (1995), Myasnikov (1997) for the two-dimensional case and in Ratkiewicz et al. (1998, 2000), Linde et al. (1998), Pogorelov and Matsuda (1998), Tanaka and Washimi (1999), Opher et al. (2003) for the three-dimensional case. Latitudinal variations of the solar wind have

been considered in Pauls and Zank (1997). The influence of the solar cycle variations on the heliospheric interface was studied in the 2D case in Steinolfson (1994), Pogorelov (1995), Karmesin et al. (1995), Baranov and Zaitsev (1998), Wang and Belcher (1999), Zaitsev and Izmodenov (2001), and in Tanaka and Washimi (1999) for the 3D case. In spite of many interesting findings in these papers, these theoretical studies did not take into account interstellar H atoms or considered the population under greatly simplified assumptions, as it was done in Linde et al. (1998), where velocity and temperature of interstellar H atoms were assumed as constants in the entire interface.

Since most of the observational information on the heliospheric interface is connected with interstellar atoms and their derivatives as pickup ions and ACRs, we will focus on models which take into account the interstellar neutral component self-consistently together with the plasma component. These models can be separated into two types. Models of the first type (Table 2.5) use a simplified fluid (or multi-fluid) approach for interstellar H atoms. A kinetic approach was used in the models of the second type. Development of the fluid (or multi-fluid) models of H atoms was connected with the fact that fluid (or multi-fluid) approach is simpler for numerical realization. At the same time such an approach can lead to nonphysical results. Results of one of the most sophisticated multi-fluid models (Zank et al., 1996) were compared with the kinetic Baranov-Malama model in Baranov et al. (1998). The comparison shows qualitative and quantitative differences in distributions of H atoms. At the same time, it was concluded in Williams et al. (1997) that the two models agreed on the distances to the termination shock, heliopause and bow shock in the upwind direction, but not in positions of the termination shock in downwind direction.

One of the common features in the models by Wang et al. (1999), Zank et al. (1996), Liewer et al. (1995), Baranov and Malama (1993), Müller et al. (2000), Myasnikov et al. (2000a,b), Aleksashov et al. (2000, 2004), Izmodenov et al. (2003a,b) is that proton, electron and pickup ion components were considered as one fluid. The great advantage of this approach is that its equations are considerably simpler as compared with the kinetic approach for pickup ions. A key assumption of this approach is immediate assimilation of pickup protons into the solar plasma. In other words, it is assumed that immediately after ionization one cannot distinguish between original solar wind protons and pickup protons. Another important assumption is that electron and proton components have equal temperatures, $T_e = T_p$. For quasineutral plasma ($n_p + n_{pui} = n_e + o(n_e)$) this means that the

pressure of the electrons is equal to half of the total plasma pressure ($P = n_e k T_e + (n_p + n_{pui}) k T_p \approx 2n_e k T_e = 2P_e$).

For the solar wind, one-fluid models assume, essentially, that wave-particle interactions are sufficient for pickup ions to assimilate quickly into the solar wind, becoming indistinguishable from solar wind protons. However, as discussed above, Voyager observations have shown that this is probably not the case. Pickup ions are unlikely to be assimilated completely. Instead, two co-moving thermal populations can be expected. A model that distinguishes the pickup ions from the solar wind ions was suggested by Isenberg (1986). Electrons were considered as a third fluid. The key assumption in the model is that pickup ions and solar wind protons are co-moving ($V_p = V_{pui}$). It was also assumed that there is no exchange of thermal energy between solar wind protons and pickup ions. Isenberg's approach consists of two continuity equations for solar protons and pickup ions; one momentum equation and three energy equations for solar wind protons, electrons and pickup ions. Note that Isenberg used the simplified form of source terms suggested in Holzer (1972) and applied these equations to the spherically symmetric solar wind upstream of the termination shock only.

Another two-fluid model of the solar wind and pickup protons was developed recently in Fahr et al. (2000). This model also assumes that convection speed of pickup ions is identical to that of solar wind protons. The pressure of the pickup ions was calculated in the model under assumption of a rectangular shape for the pickup ion isotropic distribution function. In this case, the pressure can be expressed through the pickup ion density ρ_i and solar wind bulk velocity V_{sw} as

$$P_{pui} = \rho_{pui} V_{sw}^2 / 5. \quad (2.11)$$

The model also includes ACR and GCR components as two separate massless fluids. Therefore, the governing plasma equations in the Fahr et al. (2000) model are i) one-fluid equations for the mixture of solar protons, pickup ions and electrons; ii) a continuity equation for pickup ions; iii) two transport equations for ACRs and GCRs. The influence of cosmic ray components was taken as described by the terms $-\nabla(P_{ACR} + P_{GCR})$ and $-\vec{V} \cdot \nabla(P_{ACR} + P_{GCR}) - \alpha P_{pui} \nabla \cdot (\vec{V})$ in the right-hand side of the momentum and energy equations, respectively. This approach used by Fahr et al. (2000) is crude in the sense that the assumption made on the shape of the distribution function does not reflect such important physical processes as adiabatic cooling, stochastic acceleration, and charge-exchange process of pickup ions with interstellar H atoms in the heliosheath. In addition, Fahr et al. (2000) used a simple one-fluid approach to describe the flow of interstellar H atoms. Currently, our Moscow group is

Table 2.5. Models with multi-fluid or kinetic approaches for interstellar H atoms

Reference	GCR	ACR	IMF	HMF	Lat. SW asym.	Solar Cycle	Pickup SW Protons	H Atoms
MULTI-FLUID APPROACH								
Liewer et al., 1995	-	-	-	-	-	+	one-fluid	one-fluid
Zank et al., 1996	-	-	-	-	-	-	one-fluid	three-fluid
Pauls and Zank, 1997	-	-	-	-	+	-	one-fluid	one-fluid
Wang and Belcher, 1999	-	-	-	-	-	+	one-fluid	one-fluid
Fahr et al., 2000	+	+	-	-	-	-	two-fluid	one-fluid
Fahr and Scherer, 2003a,b	+	+	-	-	-	+	two-fluid	one-fluid
KINETIC APPROACH								
Osterbart and Fahr, 1992	-	-	-	-	-	-	No pickup ions	not self-consistent
Müller et al., 2000	-	-	-	-	-	-	one-fluid	particle mesh code
Moscow team models:								
Baranov and Malama, 1993	-	-	-	-	-	-	one-fluid	Monte Carlo with splitting
Myasnikov et al., 2000a,b	+	-	-	-	-	-	one-fluid	Monte Carlo with splitting
Aleksashov et al., 2000	-	-	+	-	-	-	one-fluid	Monte Carlo with splitting
Izmodenov et al., 2003a	-	-	-	-	-	+	one-fluid	Monte Carlo with splitting
Alexashov et al., 2004	-	+	-	-	-	-	one-fluid	Monte Carlo with splitting
Malama et al., 2004	-	-	-	-	-	-	two-fluid	Monte Carlo with splitting

developing a multi-component model which is free of these limitations (Malama et al., in preparation, 2004). The kinetic equation for the H atom component will be solved self-consistently with the total plasma mass, momentum and energy equations, and the kinetic equation for pickup ion component.

5. Self-Consistent Two-Component Model of the Heliospheric Interface and Recent Advancements of the Model

The first self-consistent model of the interaction of the two-component (plasma and H atoms) LIC with the solar wind was developed by Baranov and Malama (1993). The interstellar wind was assumed to be a uniform parallel flow. The solar wind was assumed to be spherically symmetric at the Earth's orbit. Under these assumptions, the heliospheric interface has an axisymmetric structure.

Plasma and neutral components interact mainly by charge exchange. However, photoionization, solar gravity and solar radiation pressure, which are especially important in the vicinity ($< 10\text{-}15$ AU) of the Sun, are also taken into account.

Kinetic and hydrodynamic approaches were used for the neutral and plasma components, respectively. The kinetic equation (2.1) for neutrals was solved together with the Euler equations for one-fluid plasma (2.2) - (2.4). The influence of the interstellar neutrals is taken into account in the right-hand side of the Euler equations that contain source terms q_1 , \vec{q}_2 , q_3 , which are integrals (2.5)-(2.6) of the H atom distribution function $f_H(\vec{V}_H)$ and can be calculated directly by a highly efficient Monte Carlo method with splitting of trajectories (Malama, 1991). The set of kinetic and Euler equations is solved by an iterative procedure, as suggested in Baranov et al. (1991). Supersonic boundary conditions were used for the unperturbed interstellar plasma and for the solar wind plasma at the Earth's orbit. The velocity distribution of interstellar atoms is assumed to be Maxwellian in the unperturbed LIC. Results of this model are discussed below, in this section.

5.1 Plasma

Interstellar atoms strongly influence the heliospheric interface structure. The heliospheric interface is much closer to the Sun in the case when H atoms are taken into account in the model, as compared to a pure gas dynamical case (Figure 2). The termination shock becomes more spherical. The Mach disk and the complicated tail shock structure,

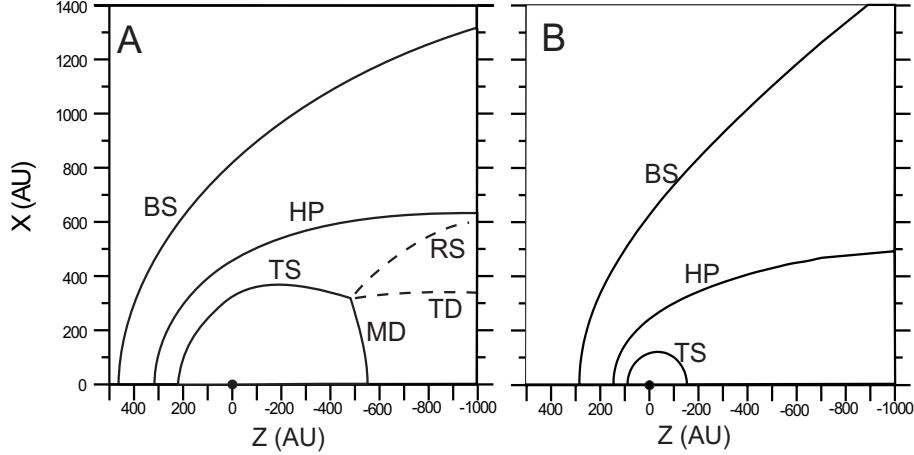


Figure 2.2. Effect of the interstellar neutrals on the size and structure of the interface structure. (a) The heliospheric interface pattern in the case of fully ionized local interstellar cloud (LIC), (b) the case of partly ionized LIC. BS is the bow shock. HP is the heliopause. TS is the termination shock. MD is the Mach disk. TD is the tangential discontinuity and RS is the reflected shock. (Izmodenov and Alexashov, 2003)

consisting of the reflected shock (RS) and the tangential discontinuity (TD), disappear.

The supersonic plasma flows upstream of the bow and termination shocks are disturbed. The supersonic solar wind flow is disturbed by charge exchange with the interstellar neutrals. The new protons created by charge exchange are picked up by the solar wind magnetic field. The Baranov-Malama model assumes immediate assimilation of pickup ions into the solar wind plasma. The solar wind protons and pickup ions are treated as one-fluid, called the solar wind. The number density, velocity, temperature, and Mach number of the solar wind are shown in Figure 3A. The effect of charge exchange on the solar wind is significant. By the time the solar wind flow reaches the termination shock, it is decelerated (15-30 %), strongly heated (5-8 times) and mass loaded (20-50 %) by the pickup ion component.

The interstellar plasma flow is disturbed upstream of the bow shock by charge exchange of the interstellar protons with secondary H atoms. These secondary atoms originate in the solar wind. This leads to heating (40-70 %) and deceleration (15-30 %) of the interstellar plasma before it reaches the bow shock. The Mach number decreases upstream of the BS and for a certain range of interstellar parameters ($n_{H,LIC} \gg n_{p,LIC}$)

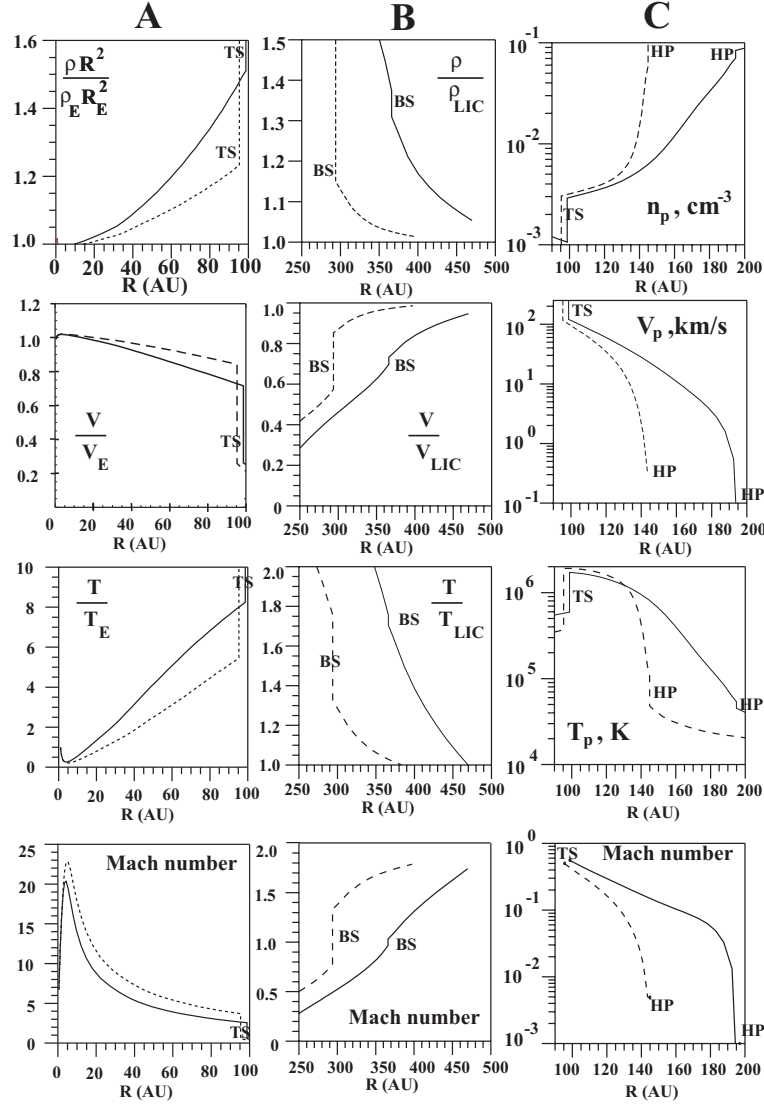


Figure 2.3. Plasma density, velocity, temperature and Mach number upstream of the termination shock (A), upstream of the bow shock (B), and in the heliosheath (C). The distributions are shown for the upwind direction. Solid curves correspond to $n_{H,LIC}=0.2 \text{ cm}^{-3}$, $n_{p,LIC}=0.04 \text{ cm}^{-3}$. Dashed curves correspond to $n_{H,LIC}=0.14 \text{ cm}^{-3}$, $n_{p,LIC}=0.10 \text{ cm}^{-3}$. $V_{LIC}=25.6 \text{ km/s}$, $T_{LIC}=7000 \text{ K}$. (Izmodenov (2000))

the bow shock may disappear. Solid curves in Figure 3B correspond to a small ionization degree in the LIC ($n_p/(n_p + n_H) = 1/6$) and the bow shock almost disappears in this case.

Interstellar neutrals also modify the plasma structure in the heliosheath. In a pure gas dynamic case (without neutrals) the density and temperature of the postshock plasma are nearly constant. However, the charge exchange process leads to a large increase in the plasma number density and decrease in its temperature (Figure 1.3C). The electron impact ionization process may influence the heliosheath plasma flow by increasing the gradient of the plasma density from the termination shock to the heliopause (Baranov and Malama, 1996). The influence of interstellar atoms on the heliosheath plasma flow is important, in particular, for the interpretations of kHz radio emission detected by Voyager (Gurnett et al., 1993; Gurnett and Kurth, 1996; Treumann et al. 1998) and possible future heliospheric imaging in energetic neutral atom (ENA) fluxes (Gruntman et al., 2001; IBEX mission).

5.2 H Atoms

Charge exchange significantly alters the interstellar atom flow. Atoms newly created by charge exchange have the velocity of their ion counterparts in charge exchange collisions. Therefore, the velocity distribution of these new atoms depends on the local plasma properties in the place of their origin. It is convenient to distinguish four different populations of atoms, depending on region in the heliospheric interface where the atoms were formed. Population 1 is the atoms created in the supersonic solar wind up to the TS. Population 2 is the atoms created in the inner heliosheath, the region between the TS and HP. Population 3 is the atoms created in the outer heliosheath - the region of disturbed interstellar wind between the HP and the BS. We will call original (or primary) interstellar atoms population 4. The number densities and mean velocities of these populations are shown in Figure 4 as functions of the heliocentric distance. The velocity distribution function of interstellar atoms $f_H(\vec{w}_H, \vec{r})$ can be represented as a sum of the distribution functions of these populations: $f_H = f_{H,1} + f_{H,2} + f_{H,3} + f_{H,4}$. The Monte Carlo method allows us to calculate these four distribution functions. The velocity distributions of the interstellar atoms at the 12 selected points in the heliospheric interface were shown by Izmodenov (2001), Izmodenov et al. (2001). As an example, the velocity distributions at the termination shock in the upwind direction are shown in Figure 5 for four introduced populations of H atoms. Note that velocity distributions of H atoms in the heliosphere were also presented by Müller et al. (2000). However, different populations of H atoms cannot be considered separately in the mesh particle simulations of H atoms (Lipatov et al., 1998) which were used in that paper.

Original (or primary) interstellar atoms are significantly filtered (i.e. their number density is reduced) before reaching the termination shock (Figure 4A). Since slow atoms have a small mean free path in comparison to fast atoms, they undergo more intensive charge exchange. This kinetic effect, called “selection”, results in a deviation of the interstellar distribution function from Maxwellian (Figure 5A). The selection also results in $\sim 10\%$ increase in the primary atom mean velocity towards the termination shock (Figure 4C).

The secondary interstellar atoms are created in the disturbed interstellar medium by charge exchange of primary interstellar neutrals with protons decelerated by the bow shock. The secondary interstellar atoms collectively make up the “H wall”, a density increase at the heliopause. The “H wall” has been predicted in Baranov et al. (1991) and detected in the direction of α Cen (Linsky and Wood, 1996). At the termination shock, the number density of secondary neutrals is comparable to the number density of the primary interstellar atoms (Figure 4A, dashed curve). The relative abundances of secondary and primary atoms entering the heliosphere vary with degree of interstellar ionization. It has been shown by Izmodenov et al. (1999b) that the relative abundance of the secondary interstellar atoms inside the termination shock is larger for the models with interstellar proton number density. The bulk velocity of population 3 is about -18 to -19 km/s. The sign “-” means that the population approaches the Sun. One can see that the velocity distribution of this population is not Maxwellian (Figure 5B). The reason for the abrupt behavior of the velocity distribution for $V_z > 0$ is that the particles with significant positive V_z velocities can reach the termination shock only from the downwind direction. The velocity distributions of different populations of H atoms were calculated in Izmodenov et al. (2001) for different directions from upwind. The fine structures of the velocity distribution of the primary and secondary interstellar populations vary with direction. These variations of the velocity distributions reflect the geometrical pattern of the heliospheric interface. The velocity distributions of the interstellar atoms can be a good diagnostics of the global structure of the heliospheric interface.

Another population of the heliospheric neutrals (population 2) is **the neutrals created in the inner heliosheath** from hot and compressed solar wind protons and pickup ions. The number density of this population is an order of magnitude smaller than the number densities of the primary and secondary interstellar atoms. This population has a minor importance for interpretation of Ly α and pickup ion measurements inside the heliosphere. However, it was recently pointed out by Chalov and Fahr (2003) that charge exchange of these atoms with solar

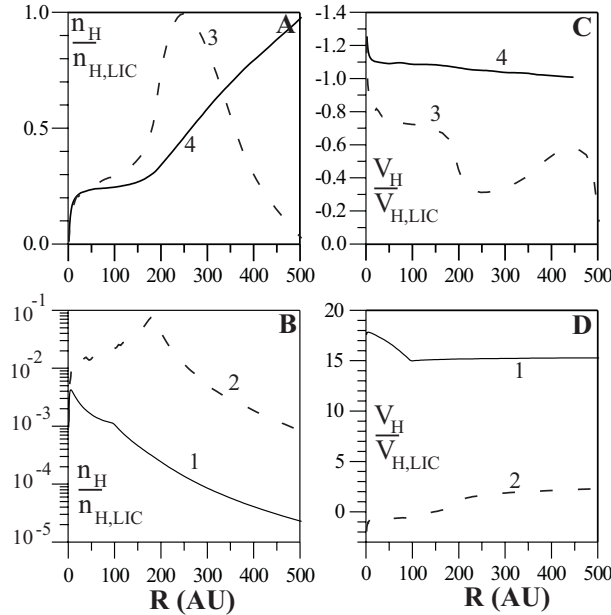


Figure 2.4 Number densities and velocities of 4 atom populations as functions of heliocentric distance in the upwind direction. 1 designates atoms created in the supersonic solar wind, 2 atoms created in the heliosheath, 3 atoms created in the disturbed interstellar plasma, and 4 original (or primary) interstellar atoms. Number densities are normalized to $n_{H,LIC}$, velocities are normalized to V_{LIC} . It is assumed that $n_{H,LIC} = 0.2 \text{ cm}^{-3}$, $n_{p,LIC} = 0.04 \text{ cm}^{-3}$. (Izmodenov et al., 2001)

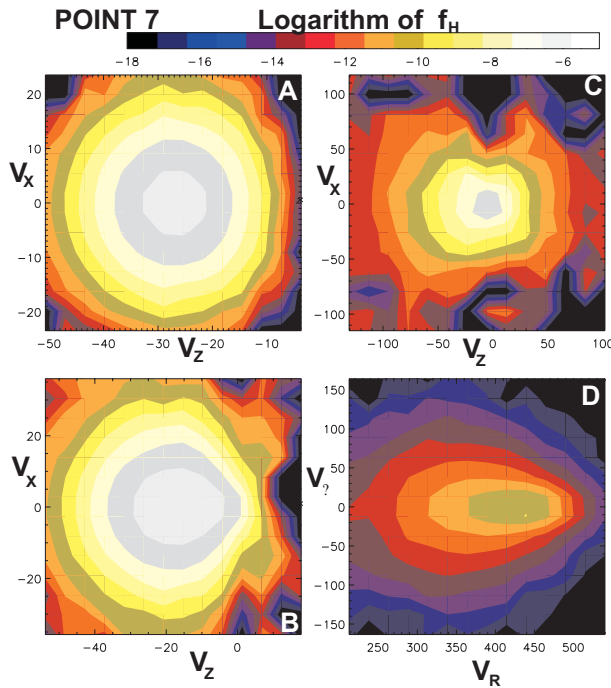


Figure 2.5 Velocity distributions of four atom populations at the termination shock in the upwind direction. (A) primary interstellar atoms, (B) secondary interstellar atoms, (C) atoms created in the heliosheath, (D) atoms created in the supersonic solar wind. V_z is the projection of velocity on the axis parallel to the LIC velocity vector. Negative values of V_z indicate approach to the Sun. V_x is the radial component of the projection of velocity vector on the perpendicular plane. V_z , V_x are in cm/sec. It is assumed that $n_{H,LIC} = 0.2 \text{ cm}^{-3}$, $n_{p,LIC} = 0.04 \text{ cm}^{-3}$. (Izmodenov et al., 2001)

wind protons produces tails in the velocity distribution of pickup ions measured at one or several AU during quiet time periods. Some atoms

of the population that may be detectable by Ly α hydrogen cell experiments due to their large Doppler shifts (Quemerais and Izmodenov, 2002). Due to their high energies and large mean free path, a portion of the atoms in this population penetrate upstream of the BS and disturb the pristine interstellar medium at large heliocentric distances. Inside the termination shock the atoms propagate freely. Thus, these atoms are a rich source of information on the plasma properties at the place of their birth, i.e. the inner heliosheath. There are plans to measure this population of atoms on future missions, including HIGO and a proposed Small Explorer called the Interstellar Boundary Explorer (IBEX) mission.

The last population of the heliospheric atoms is **the atoms created in the supersonic solar wind**. The number density of this atom population has a maximum at ~ 5 AU. At this distance, the number density of the population is about two orders of magnitude smaller than the number density of interstellar atoms. Outside the termination shock the density decreases faster than $1/r^2$, where r is the heliocentric distance (curve 1, Figure 4B). The mean velocity of population 1 is about 450 km/sec, which corresponds to the bulk velocity of the supersonic solar wind. The velocity distribution of this population is also not Maxwellian (Figure 5D). The extended “tail” in the distribution function is caused by the solar wind plasma deceleration upstream of the termination shock. This “supersonic” atom population penetrates the interface and charge exchanges with interstellar protons beyond the BS. The process of charge exchange leads to heating and deceleration upstream of the bow shock and, therefore, to the decrease of the Mach number ahead of the bow shock.

The Baranov-Malama (1993) model takes into account essentially two interstellar components: H atoms and charged particles. To apply this model to space experiments, one needs to evaluate how other possible components of the interstellar medium influence the results of this two-component model. Recently, several effects were taken into account in the frame of this axisymmetric model.

5.3 Effects of Interstellar and Solar Wind Ionized Helium

Recent measurements of interstellar helium atoms (Witte et al., 1996; Witte, 2004) and interstellar He pickup ions (Gloeckler and Geiss, 2001; Gloeckler et al., 2004) inside the heliosphere, as well as of the interstellar helium ionization (Wolff et al., 1999) allow us to estimate the number density of interstellar helium ions to be 0.008-0.01 cm^{-3} . Cur-

Table 2.6. Sets of model parameters and locations of the TS, HP and BS in the upwind direction

#	$n_{H,LIC}$ cm^{-3}	$n_{p,LIC}$ cm^{-3}	$\frac{n_{\alpha,sw}}{n_{e,sw}}$ %	HeII/(HeI+HeII)	R(TS) AU	R(HP) AU	R(BS) AU
1	0.18	0.06	0	0	95.6	170	320
2	0.18	0.06	0	0.375	88.7	152	270
3	0.18	0.06	2.5	0	100.7	176	330
4	0.18	0.06	2.5	0.150	97.5	168	310
5	0.18	0.06	2.5	0.375	93.3	157	283
6	0.18	0.06	4.5	0.375	97.0	166	291
7	0.20	0.04	0	0	95.0	183	340
8	0.20	0.04	2.5	0.375	93.0	171	290

rent estimates of the proton number density in the LIC fall in the range 0.04 - 0.07 cm^{-3} . Since helium ions are four times heavier than protons the dynamic pressure of the ionized helium component is comparable to the dynamic pressure of the ionized hydrogen component. Therefore, interstellar ionized helium cannot be ignored in the modeling of the heliospheric interface. For the first time, effects of interstellar ionized helium were studied by Izmodenov et al. (2003b). Simultaneously with interstellar ionized helium, the paper took into account solar wind alpha particles, which constitute 2.5 - 5 % of the solar wind and, therefore, produce 10 - 20 % of the solar wind dynamic pressure.

To evaluate possible effects of both interstellar ions of helium and solar wind alpha particles Izmodenov et al. (2003b) performed parametric model calculations with the eight sets of boundary conditions given in Table 2.6. Calculated locations in the upwind direction of the termination shock, the heliopause, and the bow shock are given for each model in the last three columns of Table 2.6. It is seen that the heliopause and the termination and bow shocks are closer to the Sun when the influence of interstellar helium ions is taken into account. This effect is partially compensated by additional solar wind alpha particle pressure that we also took into account in our model. The net result is as follows: the heliopause, termination and bow shocks are closer to the Sun by ~ 12 AU, ~ 2 AU, ~ 30 AU, respectively in the model taking into account both interstellar helium ions and solar wind alpha particles (model 5) as compared to the model ignoring these ionized helium components (model 1). It was also found that both interstellar ionized helium and solar wind alpha particles do not influence the filtration of the interstellar H atoms through the heliospheric interface.

5.4 Effects of GCRs, ACRs and the Interstellar Magnetic Field

The influence of the galactic cosmic rays on the heliospheric interface structure was studied by Myasnikov et al. (2000a,b). The study was done in the frame of two-component (plasma and GCRs) and three-component (plasma, H atoms and GCRs) models. For the two-component case it was found that cosmic rays could considerably modify the shape and structure of the solar wind termination shock and the bow shock and change heliocentric distances to the heliopause and the bow shock. At the same time, for the three-component model it was shown that the GCR influence on the plasma flows is negligible when compared with the influence of H atoms. The exception is the bow shock, a structure that can be strongly modified by the cosmic rays. The dynamical influence of ACRs on the solar wind flow in the outer heliosphere and on the structure of the termination shock has been studied by Fahr et al. (2000) and Alexashov et al. (2004). Whereas earlier research on the cosmic-ray-modified heliosphere was devoted mainly to the dependence of the termination shock structure and position on the injection rate of ACRs, Alexashov et al. (2004) studied effects connected with changes in the value of the diffusion coefficient while keeping the injection rate fixed. Different values of the diffusion coefficient were considered for the reason that K is poorly known in the outer heliosphere and especially in the heliosheath, and in addition the value of the diffusion coefficient varies with the solar cycle. It was shown that: 1. The effect of ACRs on the solar wind flow near the termination shock leads to formation of a smooth precursor, followed by the subshock, and to a shift of the subshock towards larger distances in the upwind direction. This result is consistent with earlier findings based on one-dimensional spherically symmetric models. Both the intensity of the subshock and the magnitude of the shift depend on the value of the diffusion coefficient, with the largest shift (about 4 AU) occurred at medium values of K . 2. The precursor of the termination shock is rather pronounced except the case with large K . It has been shown by Berezhko (1986), Chalov (1988a, 1988b), and Zank et al. (1990) that the precursor of a cosmic-ray-modified shock is highly unstable with respect to magnetosonic disturbances if the cosmic-ray pressure gradient in the precursor is sufficiently large. The possible detection of oscillations in the magnetic field and solar wind speed by the Voyager spacecraft in the near future could be considered as evidence for the termination shock. The oscillations connected with the instability of the precursor have a distinctive feature: the magnetic field in more unstable modes oscillates in the longitudinal direction, while the solar

wind speed oscillates in the direction perpendicular to the ecliptic plane (Chalov, 1990). 3. The postshock temperature of the solar wind plasma is lower in the case of the cosmic-ray-modified termination shock when compared with the shock without ACRs. The decrease in the temperature results in a decrease in the number density of hydrogen atoms originating in the region between the termination shock and heliopause. 4. The cosmic-ray pressure downstream of the termination shock is comparable to the thermal plasma pressure for small K when the diffusive length scale is much smaller than the distance to the shock. On the other hand, at large K the postshock cosmic-ray pressure is negligible when compared with the thermal plasma pressure. There is pronounced upwind-downwind asymmetry in the cosmic-ray energy distribution due to a difference in the amount of the energy injected into ACRs in the up- and downwind parts of the termination shock. This difference in the injected energy is connected with the fact that the thermal plasma pressure is lower in the downwind part of the shock when compared with the upwind part.

Effects of the interstellar magnetic field on the plasma flow and on distribution of H atoms in the interface were studied in Aleksashov et al. (2000) in the case of magnetic field parallel to the relative Sun/LIC velocity vector. In this case, the model remains axisymmetric. It was shown that effects of the the interstellar magnetic field on the positions of the termination and bow shocks and the heliopause are significantly smaller when compared to model with no H atoms (Baranov and Zaitsev, 1995). The calculations were performed with various Alfvén Mach numbers in the undisturbed LIC. It was found that the bow shock straightens out with decreasing Alfvén Mach number (increasing magnetic field strength in LIC). It approaches the Sun near the symmetry axis, but recedes from it on the flanks. By contrast, the nose of the heliopause recedes from the Sun due to tension of magnetic field lines, while the heliopause in its wings approaches the Sun under magnetic pressure. As a result, the region of compressed interstellar medium around the heliopause (or “pileup region”) decreases by almost 30 %, as the magnetic field increases from zero to 3.5×10^{-6} Gauss. It was also shown in Aleksashov et al. (2000) that H atom filtration and heliospheric distributions of primary and secondary interstellar atoms are virtually unchanged over the entire assumed range of the interstellar magnetic field (0 - $3.5 \cdot 10^{-6}$ Gauss). The magnetic field has the strongest effect on the density distribution of population 2 of H atoms, which increases by a factor of almost 1.5 as the interstellar magnetic field increases from zero to $3.5 \cdot 10^{-6}$ Gauss.

5.5 Effects of the Solar Cycle Variations of the Solar Wind

More than 30 years' (three solar cycles) observations of the solar wind show that its momentum flux varies by factor of ~ 2 from solar maximum to solar minimum (Gazis, 1996; Richardson, 1997). It has been shown theoretically that such variations of the solar wind momentum flux strongly influence the structure of the heliospheric interface - the region of the solar wind interaction with the local interstellar medium (e.g., Karmesin et al., 1995; Wang and Belcher, 1999; Baranov and Zaitsev, 1998; Zank, 1999b; Zaitsev and Izmodenov, 2001; Scherer and Fahr, 2003; Zank and Müller, 2003).

Most global models of solar cycle effects ignored the interstellar H atom component or took this component into account by using simplified fluid approximations. These simplifications were done because it is difficult to solve 6D (time, two dimensions in space, and three dimensions in velocity-space) kinetic equation for the interstellar H atom component.

Recently we developed the non-stationary, self-consistent model of the heliospheric interface and used it to explore the solar cycle variations of the interface (Izmodenov et al., 2003a; Izmodenov et al., 2004b). We obtained the periodic solution of the system of Euler equations for plasma, and the kinetic equation for interstellar H atoms with the periodic boundary conditions for the solar wind at the Earth's orbit. Izmodenov et al. (2003a) presented results of the model, where the IMP 8 solar wind data were used as boundary conditions at the Earth's orbit. Detailed theoretical study of the solar cycle effects on the structure of the heliospheric interface was reported by Izmodenov et al. (2004b), where the solar wind dynamic pressure was sinusoidally varied by a factor of two over an 11-year period.

The basic results can be summarized as follows. The discontinuities vary sinusoidally with the 11-year period dictated by the inner boundary conditions. The termination shock varies within ± 7 AU over the solar cycle in the upwind direction. Fluctuations of the TS become larger as we go from upwind to downwind. The variation of the TS in the downwind direction is 25 AU from its minimal to maximal value. The upwind fluctuation of the TS is nearly in anti-phase with its downwind fluctuations. The heliopause fluctuates with a smaller (~ 3 AU) amplitude when compared to the TS. The fluctuation of the BS with the solar cycle is less than 0.1 AU in upwind. The mean solar-cycle value of the locations of the TS, HP and BS are very close to their values obtained in the stationary model with solar cycle averaged boundary conditions.

The strength of the TS has important consequences for anomalous cosmic rays (ACRs), because the velocity jump at the TS relates to the spectral index of ACRs, β , where the intensity of the cosmic rays j varies with energy E as $j \sim E^\beta$. Izmodenov et al. (2004b) have computed the solar cycle variation of the velocity jump at the TS. The upwind jump varies insignificantly, from 2.92 to 3.09, and from 2.92 to 3.17 downwind.

Plasma parameters perform 11-year fluctuations in the entire computation region. However, the wave-length of the plasma fluctuations in the solar wind is large when compared with the distances to the TS and HP in the upwind direction. Large-scale waves are also seen in plasma distributions of the post-shocked plasma in the downwind region. Amplitudes of the waves are much less than in the upwind direction and the wavelength is ~ 200 AU. The situation is different in the outer heliosheath, the region between the HP and BS. Motion of the heliopause produces a number of shocks and rarefaction waves. The amplitudes of these shocks and rarefaction waves decreases while they propagate away from the Sun due to the increase of their surface areas and interaction between the shocks and rarefaction waves. The characteristic wavelength is ~ 40 AU. It was shown also that the 11 year averaged distributions of plasma parameters practically coincides with plasma parameters obtained in stationary model with 11 year average boundary conditions.

For interstellar H atoms, Izmodenov et al. (2004b) obtained the following results. A clear 11-year periodicity is seen in the fluctuations of H atom densities. Deviations from exact 11-year sinusoidal periodicity are connected with errors of our statistical calculations, which are ~ 2 -3%. In the outer heliosphere and, in particular, at the TS the variations of densities are within $\pm 5\%$ of their mean value for primary and secondary interstellar populations and for the populations of atoms created in the inner heliosheath. Closer to the Sun, for distances < 10 AU, the amplitude of fluctuations increases up to $\pm 15\%$ around the mean value. The variation of the number density of H atoms created in the supersonic solar wind is $\pm 30\%$ of the mean value. Variations of mean velocity and kinetic temperature of primary and secondary interstellar atoms are negligibly small for both interstellar populations, in comparison to statistical uncertainty. However, the mean velocity and kinetic temperature of atoms created in the inner heliosheath vary with the solar cycle by 10-12%. This is connected with the fact that the most of the H atoms of the latter population are created in the vicinity of the heliopause and they reflect the long wavelength plasma variations in this region.

It is important to note that number densities of the three components (primary and secondary interstellar populations, and the population of H

atoms created in the inner heliosheath) fluctuate in phase. This coherent behavior of the fluctuations exists in all supersonic solar wind regions for the three populations and, also, in the inner heliosheath for the primary and secondary atoms. The reason of such coherent behavior of the variations of H atom densities becomes evident when the fluctuations are compared with plasma density variations (see, Izmodenov et al., 2004b). The two variations are almost in anti-phase. Apparently, such a correlation is only possible when temporal variations of the H atom densities are caused by variation of the local loss of the neutrals due to the charge exchange and ionization processes.

However, coherent fluctuations of different populations of H atoms disappear in the regions where the populations originate and the process of creation is dominant when compared with the losses. Indeed, in the inner heliosheath fluctuations of number density of H atoms created in this region are shifted as compared with coherent fluctuations of primary and secondary interstellar atom populations and are in phase with variations of proton number density near the heliopause. Variations of the secondary interstellar atom population are in anti-phase with variations of primary atoms in the outer heliosheath and almost in phase with plasma fluctuations in the region. Again, the creation process is dominant in the outer heliosheath for the population of secondary interstellar atoms.

It is important to note that the above described behavior of H atom populations in the heliospheric interface is kinetic in nature. Variations are determined basically by loss and creation processes, but not by convection and pressure gradient terms as it would be in fluid or multi-fluid approaches. The validity of fluid approach is determined by the simple criterium that the Knudsen number $Kn = l/L \ll 1$, where l and L are the mean free path of the particles and characteristic size of the problem, respectively. For stationary problems, the distance between the HP and BS, which is approximately 100 AU, can be chosen as characteristic size. The mean free path of H atoms in the region is ~ 50 AU (Izmodenov et al., 2000). Therefore, $Kn_{stationary} \approx 0.5$. As was described above, kinetic and fluid approaches were compared by Baranov et al. (1998) and Izmodenov et al. (2001), showing explicitly that the velocity distribution function of H atoms is not Maxwellian anywhere in the interface. For the time-dependent problem considered in this section, the characteristic size, L , is half of the wavelength in the plasma distributions. In the region between the HP and BS, $L \approx 20$ AU. Therefore, $Kn_{time} \approx 2.5$ and fluid approaches become even less appropriate when compared with stationary models. This fundamental point could be the main reason for the large difference between results presented by Izmodenov et al.

(2004b) and results obtained by Zank and Müller (2003) and Scherer and Fahr (2003a,b) who used multi-fluid approaches.

5.6 Heliotail

Plasma and H atom distributions in the tail of the LIC/SW interaction region were not of interest up until recently. However, modeling of the heliospheric interface gives answers to the two fundamental questions: 1. Where is the edge of the solar system plasma? 2. How far downstream can the influence of the solar wind be felt on the surrounding interstellar medium?

To supply an answer to the first question we need to define the solar plasma system boundary. It is natural to assume the heliospheric boundary is the heliopause that separates the solar wind and interstellar plasmas. This definition is not completely correct, because the heliopause is an open surface and, therefore, the heliosphere ends at infinity. To resolve the problem, and to address the second question, detailed specific modeling of the structure of the tail region up to 50000 AU was performed by Izmodenov and Alexashov (2003), Alexashov and Izmodenov (2003), Alexashov et al. (2004). It was shown that the charge exchange process qualitatively changes the solar wind - interstellar wind interaction in the tail region. The termination shock becomes more spherical and the Mach disk, reflected shock and tangential discontinuity disappear. This result was obtained previously by Baranov and Malama (1993), who performed calculations up to 700 AU in the heliotail. In addition, Alexashov et al. (2004) found that the jumps of density and tangential velocity across the heliopause become smaller in the heliotail and disappear at about 3000 AU. Parameters of solar wind plasma and interstellar H atoms approach their interstellar values at large heliocentric distances. This allows an estimation of the influence of the solar wind, and, therefore, the solar system size in the downwind direction to about 20,000 - 40,000 AU. An illustration of the results is shown in Figure 6. The figure shows isolines of the Mach number up to 10,000 AU. The solar wind plasma has a velocity 100 km/s and a temperature of $1.5 \cdot 10^6$ K immediately after passing the TS. Then the velocity becomes smaller due to new protons injected by charge exchange and approaches the value of interstellar velocity. Since interstellar H atoms are effectively cooler when compared with postshocked protons, the solar wind also becomes cooler. This makes the Mach number increase. At distances of 4,000 AU the solar wind again becomes supersonic and the Mach number then approaches its interstellar value at 40,000 - 50,000 AU, where the solar wind gas dynamic parameters become undistin-

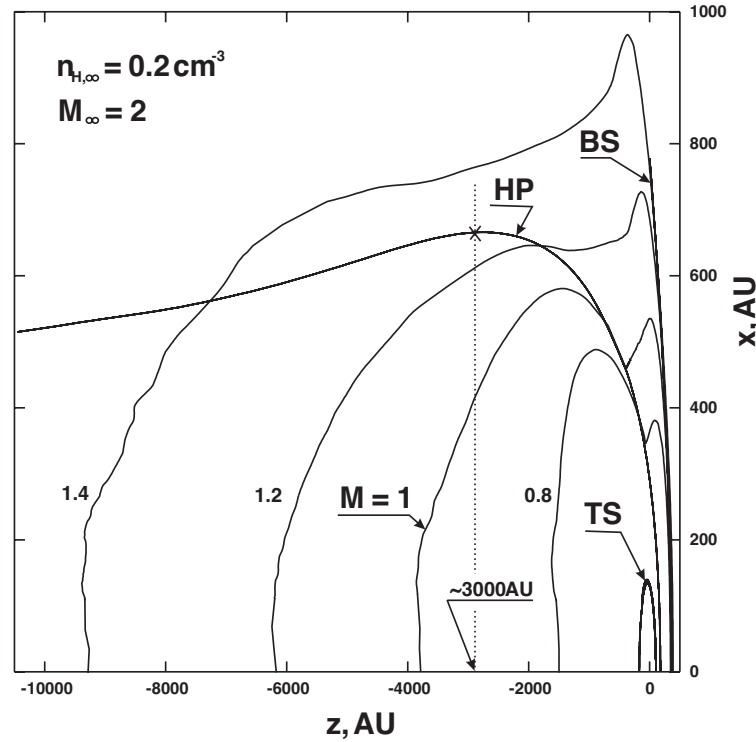


Figure 2.6. Isolines of Mach number of solar wind and interstellar plasma flows in the downwind direction (Alexashov et al., 2004).

guishable from undisturbed interstellar parameters. This result cannot be obtained in the absence of H atoms because the solar wind flow in the heliotail remains subsonic in that case.

6. Interpretations of Spacecraft Experiments Based on the Heliospheric Interface Model

As it was stated in Section 2, the Sun/LIC relative velocity and the LIC temperature are now well constrained (Witte et al., 1996; Witte, 2004; Lallement and Bertin, 1992; Linsky et al., 1993; Lallement et al., 1995, 1996; Moebius et al., 2004). To obtain other interstellar parameters one needs to use one or several remote diagnostics of the interface and a theoretical model.

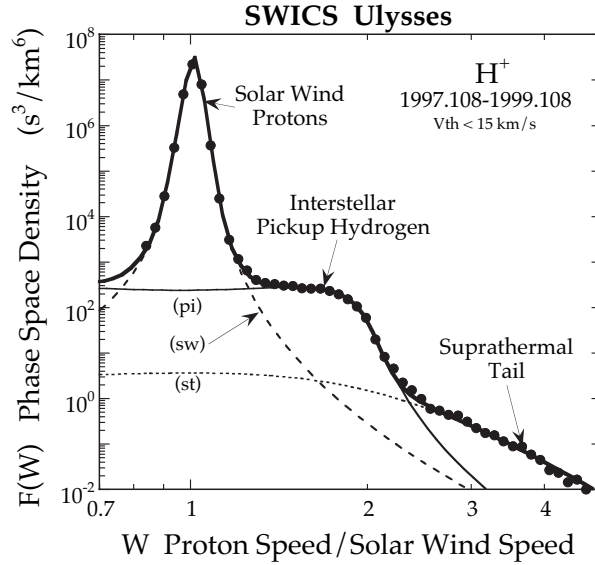


Figure 2.7. Two-year-averaged phase space density of H^+ versus normalized speed W (proton speed divided by solar wind speed) observed with the Solar Wind Ion Composition Spectrometer (SWICS) on Ulysses in the slow solar wind at ~ 5 AU and low latitude. Only quiet-time periods, characterized by a low solar wind thermal speed (< 15 km/s) were used in this average. Interstellar pickup hydrogen is the dominant component in the flat portion of the spectrum between $W \sim 1.3$ and ~ 2.2 . Solar wind protons, modeled by curve (sw), dominate below $W \sim 1.3$ and accelerated protons form the suprathermal tail above $W \sim 2.2$, modeled by curve (st). During quiet time periods used here, the solar wind distribution is sufficiently narrow and the suprathermal tail sufficiently weak, to reveal more fully the pickup ion component of the spectrum. The curve labeled (pi) is computed using model parameters given in the text. The atomic hydrogen density at the termination shock is found to be $0.100 \pm 0.008 \text{ cm}^{-3}$ (Izmodenov et al., 2003a).

6.1 Pickup ions

The charge exchange process in the heliospheric interface leads to a predictable reduction, or filtration, of interstellar atomic hydrogen that enters the heliosphere. The most accurate determination of the density of interstellar H atoms inside the heliosphere comes from measurements of pickup H^+ . An example of a typical proton velocity distribution is given in Figure 7 (Figure 2, Izmodenov et al., 2003a; see also Gloeckler and Geiss, 2001). This spectrum was observed with the Solar Wind Interstellar Composition Spectrometer (SWICS) on Ulysses in the slow solar wind at ~ 5 AU during quiet times at low latitudes.

The pickup ion distribution (labeled 'pi' in Figure 7) is modelled by using the “hot model” of Thomas (1978) for the spatial distribution of hydrogen atoms in the heliosphere and equations (9) and (10b) of Vasyliunas and Siscoe (1976) derived under the assumption of rapid pitch-angle scattering and hence isotropy the phase-space density of the resulting pickup protons. Model parameters, in particular the neutral hydrogen density at the termination shock, are adjusted until the best fit to the measured spectrum is obtained. The assumption of isotropic pickup ion distributions is justified in this case because at 5 AU in the ecliptic plane the average magnetic field direction is nearly perpendicular to the solar wind flow direction.

Heliospheric parameters affecting the model pickup ion distribution are known from direct measurements. During the 2-year time period of Figure 7 the average photoionization rate for hydrogen, derived from Lyman alpha measurements on SOHO was $0.8 \times 10^{-7} \text{ s}^{-1}$ (D. R. McMullin and D. L. Judge, priv. comm.). The ionization rate from charge exchange, a product of solar wind flux (measured with SWICS) and charge exchange cross section was $5.4 \times 10^{-7} \text{ s}^{-1}$, giving a total loss rate of $6.2 \times 10^{-7} \text{ s}^{-1}$. The total production rate of pickup hydrogen is somewhat smaller ($5.1 \times 10^{-7} \text{ s}^{-1}$) because the average solar wind flux for time periods of low thermal speed was measured to be lower than for the entire two year time period. With these values for the loss and production rates, an excellent fit to the measured pickup proton distribution is obtained and the number density of atomic H at the termination shock is determined to be $0.100 \pm 0.005 \text{ cm}^{-3}$. The number density can be compared with the number density at the TS obtained in the theoretical models. Izmodenov et al. (2003b) used the heliospheric interface model, which was described above and takes into account influence of both interstellar and solar ionized helium. Parametric studies were performed in that paper by varying the interstellar proton and hydrogen atom number densities in the ranges of 0.03- 0.1 and 0.16 - 0.2 cm^{-3} , respectively. Figure 8 shows updated results compared with the calculations presented in Izmodenov et al. (2003a). Red curves are isolines of H atom number density at the TS. The dashed red area shows the range of possible pairs of $(n_{H,LIC}, n_{p,LIC})$, which are comparable to $n_{H,TS}$ obtained from pickup ions data. To reduce the range of possible interstellar atom and proton densities we need to employ other observational diagnostics. These could include, for example, the interstellar helium ionization ($\chi(He) = n_{He^+,LIC}/(n_{He^+,LIC} + n_{He,LIC})$) range of 0.3-0.4 derived from line-of-sight Extreme Ultraviolet Explorer measurements toward white dwarf stars in the local interstellar medium (Wolff et al. 1999). Using 1) ULYSSES/GAS measurements of the LIC

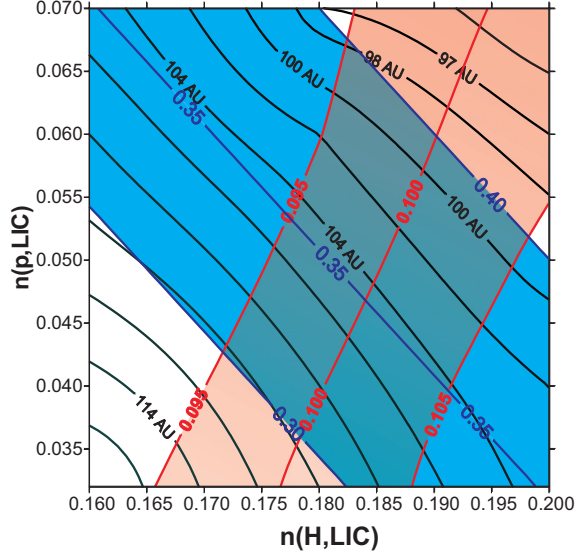


Figure 2.8 Contour plots of the interstellar H atom number density at the termination shock, the LIC helium ionization fraction, and the termination shock location in the Voyager direction.

atomic He density ($= 0.015 \text{ cm}^{-3}$; Gloeckler and Geiss 2001; Witte, priv. comm.), 2) the standard universal ratio of the total H to He, $(n_{p,LIC} + n_{H,LIC}) / (n_{He^+,LIC} + n_{He,LIC}) = 10$, the relation between $n_{H,LIC}$ and $n_{p,LIC}$ can be established with

$$n_{p,LIC} + n_{H,LIC} = 0.15(1 - \chi(He^+))^{-1}, \text{ cm}^{-3}.$$

Isolines of interstellar helium ionization $\chi(He^+)$ are shown in Figure 8. The intersection of the two shaded areas gives the most likely values of interstellar proton and atomic hydrogen number densities compatible with the observations: $n_{H,LIC} = 0.185 \pm 0.01 \text{ cm}^{-3}$ and $n_{p,LIC} = 0.05 \pm 0.015 \text{ cm}^{-3}$. The interstellar hydrogen ionization fraction derived from this result is in agreement with recent calculations of the photoionization of interstellar matter within 5 pc of the Sun (Slavin and Frisch, 2002).

6.2 Location of the Termination Shock in the Direction of Voyager 1

Based on measurements of the low-energy particle fluxes, spectra, and composition by the Voyager 1 Low Energy Charged Particle instrument and of an indirect determination of the solar wind speed using particle anisotropy measurements, Krimigis et al. (2003) reported the probable crossing of the TS by Voyager 1 at 85 AU in the summer of 2002 and the return to the TS upstream region about 6 months later. McDonald et al. (2003) suggested another interpretation of the Voyager data arguing that the spacecraft remained in the supersonic wind, but in the precursor region. In any case, recent Voyager 1 data suggest that the TS was

close to 85 AU in the Voyager 1 direction. To compare this evidence with model predictions we plot in Figure 8 isolines of the distance to the TS in the middle of 2002, computed in the Voyager direction. It is seen that for $(n_{H,LIC}, n_{p,LIC})$ comparable to the ionization range of interstellar helium of 0.3 - 0.4 the TS location is 104 ± 4 AU, which is ~ 20 AU farther from the Sun than Voyager 1. One possible solution to get the TS at ~ 85 AU in the model is to increase the interstellar atom and proton number densities. Our model-calculations show that for $n_{p,LIC} = 0.11 - 0.12 \text{ cm}^{-3}$ and $n_{H,LIC} \approx 0.22 \text{ cm}^{-3}$ the TS was at 85-86 AU in 2002 and the number density of H atoms at the TS is $\sim 0.1 \text{ cm}^{-3}$. However, such a solution implies 55 % interstellar helium ionization.

6.3 Filtration of Interstellar Oxygen and Nitrogen

Additional constraints on the local interstellar properties and, in particular, local interstellar abundances can be obtained using measurements of pickup ions of heavier interstellar atoms made by Ulysses/SWCIS (Gloeckler and Geiss, 2001) and theoretical calculations of filtration of the atoms through the heliospheric interface.

Izmodenov et al. (2004a) performed comparative studies of the penetration of the interstellar atoms of H, O, N into the heliosphere through the heliospheric interface. We made a parametric study by varying local interstellar proton and atom number densities. It was found that $54 \pm \%$ of interstellar hydrogen atoms, $68 \pm 3 \%$ of interstellar oxygen and $78 \pm 2 \%$ of interstellar nitrogen penetrate through the interaction region into the interface. In the case of a lower electron temperature in the heliosheath $81 \pm 2 \%$ and $89 \pm 1 \%$ of interstellar oxygen and nitrogen penetrate, respectively. Using our filtration coefficients and SWICS Ulysses pickup ion measurements we conclude that $n_{OI,LIC} = (7.8 \pm 1.3) \cdot 10^5 \text{ cm}^{-3}$ and $n_{NI,LIC} = (1.1 \pm 0.2) \cdot 10^5 \text{ cm}^{-3}$. Finally, the local interstellar OI to HI and NI to OI ratios are $(OI/HI)_{LIC} = (4.3 \pm 0.5) \cdot 10^4$ and $(NI/OI)_{LIC} = 0.13 \pm 0.01$. Our interstellar OI/HI ratio is slightly lower than the ratio $(4.8 \pm 0.48) \cdot 10^4$ determined by Linsky et al. (1995) from spectroscopic observations of stellar absorption.

7. Summary

The Local Interstellar Medium interacts with the solar wind and influences the outer heliosphere in a complicated way. Several particle populations and magnetic fields are involved in this interaction. From the interstellar side, the interacting populations are the plasma (electron and

proton) component, H atom component, interstellar magnetic field, and galactic cosmic rays. Heliospheric plasma consists of the original solar wind protons, electrons, pickup protons, and the anomalous component of cosmic rays. A large effort has been made to study the theoretical physics of the interaction region. However, a complete, self-consistent model of the heliospheric interface has not yet been constructed, because of the difficulty incorporating both the multi-component nature of the heliosphere and the requirement for different theoretical approaches for different components of the interaction. Many aspects were studied and reported here. However, some aspects require additional theoretical exploration. Most of the theoretical models employ the one-fluid approach for solar wind and interstellar plasmas. It has been shown that several assumptions are needed to derive one-fluid approach equations. A key assumption that looks reasonable is that invoking a co-moving character for all components. Another assumption for a one-fluid plasma model is the immediate assimilation of the pickup ion component into the solar wind. As demonstrated by space experiments, this is not the case and it would be more natural to consider solar protons and pickup protons as separate co-moving populations. The electron component should also be treated as a distinct population. However, since the assumption of the co-moving character of these three heliospheric plasma populations looks reasonable to order one, the one-fluid approach gives us a reasonably accurate picture of the flow pattern (positions of the shocks and heliopause) and plasma velocity distributions. Theoretical kinetic models of the pickup ion transport and acceleration can be employed to determine the distribution of thermal energy between the solar wind and pickup proton components. A similar study should be done for electrons.

Finally, growing interest in heliospheric interface studies is connected with expectations that Voyager 1 recently crossed the termination shock or will cross the shock in the near future. Many predictions of the time of the termination shock being crossed by Voyager appeared in the literature. However, it seems that much more work should be done to explain and reconcile all available indirect observations of the heliospheric interface based on the unique model of the heliospheric interface. This work should be done especially because NASA plans to explore the interaction region remotely by ENA imaging (HIGO, or the proposed Small Explorer Mission known as IBEX, Web-page at <http://ibex.swri.edu/>) and to send a spacecraft (the Interstellar Probe) to a heliocentric distance of at least 200 AU with a flight-time of only 10 or 15 years (<http://interstellar.jpl.nasa.gov/>). Intensive theoretical study will help to optimize goals, instrumentation, and, finally, the scientific profit of the “interstellar” missions.

Acknowledgements. This work was supported in part by INTAS Award 2001-0270, RFBR grants 04-02-16559, 03-01-39004, 03-02-04020, 04-01-00594 and the International Space Science Institute in Bern. I thank Steve Suess for his numerous corrections and suggestions to improve style and English of the paper. I also thank Sergey Chalov for useful discussions.

References

- Aleksashov, D., Baranov, V., Barsky, E., Myasnikov, A., *Astronomy Letters*, 26 (2000), 743-749.
- Alexashov, D. and V. Izmodenov, in SOLAR WIND TEN: Proceedings of the Tenth International Solar Wind Conference, Eds. M. Velli and R. Bruno, AIP Conference Proceedings 679, pp. 218-221, 2003.
- Alexashov, D., V.V. Izmodenov and S. Grzedzielski, *Adv. Space Res.*, in press, 2004.
- Alexashov, D., Chalov, S.V., Myasnikov, A., Izmodenov V., Kallenbach, R., *Astron. Astrophys.*, in press, 2004.
- Baranov, V.B., Krasnobaev, K.V., Kulikovksy, A.G., *Sov. Phys. Dokl.* 15 (1971), 791.
- Baranov, V. B., Lebedev, M., Malama Y., *Astrophys. J.* 375 (1991), 347-351.
- Baranov, V., Malama, Y., *J. Geophys. Res.* 98 (1993), 15157.
- Baranov, V. B., Malama, Y. G., *J. Geophys. Res.* 100 (1995), 14,755-14,762.
- Baranov, V.B., Zaitsev, N.A., *Astron. Astrophys.* 304 (1995), 631.
- Baranov, V., Zaitsev, N., *Geophys. Res. Let.* 25 (1998), 4051.
- Baranov, V. B., Izmodenov, V., Malama, Y., *J. Geophys. Res.* 103 (1998), 9575-9586.
- Baranov, V. B., *Astrophys. Space Sci.* 274 (2000), 3-16.
- Baranov, V. B., and Y. G. Malama, *Space Sci. Rev.* 78 (1996), 305-316.
- Baranov, V. B., and Fahr, H. J., *J. Geophys. Res. (Space Physics)*, Vol. 108,A3, pp. SSH 4-1, CiteID 1110, DOI 10.1029/2001JA009221, 2003a.
- Baranov, V. B., and H. J. Fahr, *J. Geophys. Res.*, 108(A12), 1439, 10.1029/2003JA010118, 2003b.
- Berezhko, E. G. 1986, *Soviet Astron. Let.*, 12, 352
- Chalov, S. V. 1988a, *Soviet Astron. Let.*, 14, 114
- Chalov, S. V. 1988b, *Astrophys. Space Sci.*, 148, 175
- Chalov, S. V. 1990, in *Physics of the Outer Heliosphere*, ed. S. Grzedzielski, & D. E. Page (Pergamon), 219.
- Chalov, S. V., Fahr, H., *Astron. Astrophys.* 311 (1996), 317-328.

- Chalov, S. V., Fahr, H., *Astron. Astrophys.* 326 (1997), 860-869.
- Chalov, S. V., Fahr, H., *Astron. Astrophys.*, 335 (1998), 746-756.
- Chalov, S. V., Fahr, H., *Solar Physics* 187, 123-144 (1999).
- Chalov, S. V., Fahr, H., *Astron. Astrophys.*, 401 (2003), L1-L4.
- Fahr, H., Kausch, T., Scherer, H., *Astron. Astrophys.* 357 (2000), 268-282.
- Fichtner, H., *Space Sci. Rev.* 95 (2001), 639-754.
- Florinski, V., and G. P. Zank, *J. Geophys. Res.*, 108(A12), 1438, doi: 10.1029/2003JA009950, 2003.
- Fujimoto Y., Matsuda, T., Preprint No. KUGD91-2, Kobe Univ., Japan, 1991.
- Gazis, P.R., *Reviews of Geophysics*, 34,4, 379-402, 1996.
- Gloeckler, *Space Sci. Rev.* 78 (1996), 335-346.
- Gloeckler, G., Fisk, L.A., Geiss, J., *Nature* 386 (1997), 374-377.
- Gloeckler, G., and Geiss, J., Joint SOHO/ACE workshop "Solar and Galactic Composition". Edited by Robert F. Wimmer-Schweingruber. Publisher: American Institute of Physics Conference proceedings vol. 598 location: Bern, Switzerland, March 6 - 9, 2001., p.281
- Gloeckler, G., Moebius, E., Geiss, J., *Astron. Astrophys.*, in press, 2004.
- Gurnett, D. A., Kurth, W., Allendorf, S., Poynter, R., *Science* 262 (1993), 199-202.
- Gurnett, D., Kurth, W., *Space Sci. Rev.* 78 (1996), 53-66.
- Gruntman et al., *J. Geophys. Res.* 106, 15767-15782 (2001).
- Holzer, J. *Geophys. Res.* 77 (1972), 5407.
- Isenberg, P., *J. Geophys. Res.* 91 (1986), 9965.
- Isenberg, P., *J. Geophys. Res.* 102 (1997), 4719-4724.
- Izmodenov, V., Lallement, R., Malama, Y., *Astron. & Astrophys.* 342 (1999a), L13-L16.
- Izmodenov V., Geiss, J., Lallement, R., et al., *J. Geophys. Res.* (1999b), 4731-4742.
- Izmodenov, V., *Astrophys. Space Sci.* 274 (2000), 55-69.
- Izmodenov, V., Malama, Y., Kalinin, A., et al., *Astrophys. Space Sci.* 274 (2000), 71-76.
- Izmodenov, V., *Space Sci. Rev.* 97 (2001): 385-388.
- Izmodenov, V., Gruntman, M., Malama, Y., *J. Geophys. Res.* 106 (2001), 10681.
- Izmodenov, V., Wood, B., and R. Lallement, *J. Geophys. Res.* 107(10), doi: 10.1029/2002JA009394, 2002.
- Izmodenov, V., Malama, Y.G., Gloeckler, G., *Geophys. Res. Lett.*, 2003a.
- Izmodenov, V., Malama, Y.G., Gloeckler, G., Geiss, J., *Astrophys. J.*, 594:L59-L62, 2003b.

- Izmodenov, V., and, D. Alexashov, *Astronomy Letters*, Vol. 29, No. 1, pp. 58-63, 2003.
- Izmodenov, V., Malama, Y.G., Gloeckler, G., Geiss, J., *Astron. Astrophys.*, 414, L29-L32, 2004a.
- Izmodenov, V., Malama, Y.G., Ruderman, M.S., *Astron. Astrophys.*, in press, 2004b.
- Karmesin, S., Liewer, P., Brackbill, J., *Geophys. Res. Lett.* 22 (1995), 1153-1163.
- Krimigis, S. M., Decker, R. B., Hill, M. E., et al., *Nature*, 426, Issue 6962, pp. 45-48 (2003).
- Lallement R., Bertin, *Astron. Astrophys.* 266 (1992), 479-485.
- Lallement, R., *Space Sci. Rev.* 78 (1996), 361-374.
- Lallement, R., Ferlet, A., et al., *Astron. Astrophys.* 304 (1995), 461-474.
- Lallement, R., Linsky, J., Lequeux, J., Baranov, V., *Space Sci. Rev.* 78 (1996), 299-304.
- Lazarus, A.J., and R.L. McNutt, Jr., in *Physics of the Outer Heliosphere*, Ed's S. Grzedzielski and D.E. Page, Pergamon (1990).
- Liewer, P., Brackbill, J., Karmesin, S., *International Solar Wind 8 Conference*, p.33, 1995.
- Linde, T., Gombosi, T., Roe, P., *J. Geophys. Res.* 103 (1998), 1889-1904.
- Linsky, J., Wood, B., *Astrophys. J.* 463 (1996), 254.
- Linsky, J., Brown A., Gayley, K., et al., *Astron. J.* 402 (1993), 694-709.
- Linsky J.L., Dipas A., Wood B.E., et al., *Astrophys. J.* 476, 366, 1995.
- Lipatov, A.S., Zank, G.P., Pauls, H.L., *J. Geophys Res.* 103, (1998), 20631-20642.
- Malama, Y. G., *Astrophys. Space Sci.*, 176 (1991), 21-46.
- McComas, D.J., Barraclough, B.L., Funsten, H.O., Gosling, J., T., et al., *J. Geophys. Res.*, 105, A5, 10419-10433, 2000.
- McComas, D.J., et al., *Space Science Rev.*, 97, 189, 2001.
- McComas, D.J., Elliot, H.A., Gosling, J.T., et al., *Geophys. Res. Letters*, 29, 9, doi:10.1029/2001GL014164, 2002.
- McDonald, F. B., Stone, E. C., Cummings, A. C., et al., *Nature*, 426, Issue 6962, pp. 48-51 (2003).
- Myasnikov, A., Preprint No. 585, Institute for Problems in Mechanics, Russian Academy of Sciences, 1997.
- Myasnikov, Izmodenov, V., Alexashov, D., Chalov, S., *J. Geophys. Res.* 105 (2000a), 5179.
- Myasnikov, Alexashov, D., Izmodenov, V., Chalov, S., *J. Geophys. Res.* 105 (2000b), 5167.
- Moebius, E., *Space Sci. Rev.* 78 (1996), 375-386.
- Müller et al., *J. Geophys. Res.*, 27,419-27,438 (2000).
- Neugebauer, M., *Rev. Geophys.* 37, 1, 107-126, 1999.

- Osterbart, R., and H. Fahr, *Astron. Astrophys.* 264 (1992), 260-269.
- Opher, M., Liewer, P.C., Gombosi, T.I., et al., *Astrophys. J.* 591 (2003) L61-L65.
- Parker, E. N., *Astrophys. J.* 134 (1961), 20-27.
- Pauls, H. and G. Zank, *J. Geophys. Res.* 102 (1997), 19779-19788.
- Pogorelov, N., *Astron. Astrophys.* 297 (1995), 835.
- Pogorelov, N., Semenov, A., *Astron. Astrophys.* 321 (1997), 330.
- Pogorelov, N., Matsuda, T., *J. Geophys. Res.* 103 (1998), 237-245.
- Quemerais, E. and V. Izmodenov, *Astronomy and Astrophysics*, v.396, p.269-281, 2002.
- Ratkiewicz, R., Barnes, A, et al., *Astron. Astrophys.* 335 (1998), 363.
- Ratkiewicz, R., Barnes, A., J. Spreiter, *J. Geophys. Res.* 105 (2000), 25,021-25,031.
- Richardson, J.D., *Geophys. Res. Lett.* 24 (1997), 2889-2892.
- Richardson, J.D., *The Outer Heliosphere: The Next Frontiers*, Edited by K. Scherer, H. Fichtner, H. Fahr, and E. Marsch, COSPAR Colloquium Series, 11. Amsterdam: Pergamon Press (2001), 301-310.
- Richardson, J.D., Wang, C., Burlaga, L.F., *Advances in Space Research*, in press, 2004.
- Slavin, J. D., and Frisch, P.C., *Astrophys. J.* 565, 364-379, 2002.
- Smith, C. W., Matthaeus, W. H., Zank, G. P., et al., *J. Geophys. Res.* 106 (2001), 8253-8272.
- Steinolfson, R.S., *J. Geophys. Res.* 99 (1994), 13,307-13,314.
- Scherer, K., Fahr, H. J., *Geophys. Res. Lett.* 30 (2003), doi: 10.1029/2002GL016073, 2003a.
- Scherer, K., and Fahr, H. J., *Annales Geophys.*, 21 (2003b), 1303-1313.
- Stone, E.C., *Science*, 293, 55-56, 2001.
- Tanaka, T., Washimi, H., *J. Geophys. Res.* 104 (1999), 12605.
- Thomas, G. E., *Ann. Rev. Earth Planet. Sci.* 6, 173, 1978.
- Treumann, R., Macek, W., Izmodenov, V, *Astron. Astrophys.* 336 (1998), L45.
- Vasyliunas, V. M. and Siscoe, G. L., *system, J. Geophys. Res.* 81, 1,247-1,252, 1976.
- Webber, W.R., Lockwood, J., McDonald, F., Heikkila, B., *J. Geophys. Res.* 106 (2001), 253-260.
- Williams, L., Zank, G., Matthaeus, W., *J. Geophys. Res.* 100 (1995), 17059-17068.
- Wang, C., Belcher, J, *J. Geophys. Res.* 104 (1999), 549-556.
- Williams, L., Hall, D. T., Pauls, H. L., Zank, G. P., *Astrophys. J.* 476 (1997), 366.
- Witte, M., Banaszekiewicz, M.; Rosenbauer, H., *Space Sci. Rev.* 78 (1996), 289-296.

- Witte, M., *Astron. Astrophys.*, in press, 2004.
- Wood, B. E., Muller, H.; Zank, G. P., *Astrophys. J.* 542 (2000), 493-503.
- Wolff, B., Koester, D., and Lallement, R., *Astron. Astrophys.*, 346, 969-978, 1999.
- Zaitsev, N., Izmodenov V., in *The Outer Heliosphere: The Next Frontiers*, Edited by K. Scherer, H. Fichtner, H. Fahr, and E. Marsch, COSPAR Colloquium Series, 11. Amsterdam: Pergamon Press (2001), 65-69.
- Zank, G. P., Axford, W.I., & McKenzie, J. F. 1990, *Astron. Astrophys.*, 233, 275.
- Zank, G., Pauls, H., Williams, L., Hall, D., *J. Geophys. Res.* 101 (1996), 21639-21656.
- Zank, G., *Space Sci. Rev.* 89 (1999a), 413-688.
- Zank, G., in *Solar Wind Nine*, edited by S.R. Habbal et al., AIP (1999b), 783-786.
- Zank, G. P., Müller, H.-R., *The dynamical heliosphere*, *J. Geophys. Res.*, 108, pp. SSH 7-1, CiteID 1240, DOI 10.1029/2002JA009689, 2003.